MODELING THE PROPAGATION, CHAIN TRANSFER AND TACTICITY IN FREE RADICAL POLYMERIZATION

by

Tuğba Furuncuoğlu

B.S., Chemistry, Boğaziçi University, 2008

Submitted to the Institute for Graduate Studies in
Science and Engineering in partial fulfillment of
the requirements for the degree of
Master of Science

Graduate Program in Chemistry
Boğaziçi University
2010

ACKNOWLEDGEMENTS

I would like to express my sincere gratitude to my thesis advisor Prof. Viktorya Aviyente for her endless support and patience throughout my studies. I would like to thank her for everything that I learned from her. It is always a great pleasure for me to be her student.

I wish to thank to the members of my committee: Prof. Turgut Nugay and Prof. Türkan Haliloğlu for giving their valuable time and advices.

I would like to thank to all the members of computational chemistry family, especially to İsa Değirmenci and İlke Uğur for their mass contributions to our project, to Gülşah Çifci, Burcu Çakır Dedeoğlu, Şeref Gül, Özlem Karahan and Sesil Agopcan. I would like to express my gratefulness to the Chemistry Department, especially to Hülya Metiner as the most helpful member of the department.

Finally, I would like to express deepest gratitude to my family for their continuous love and support throughout my life.

ABSTRACT

MODELING THE PROPAGATION, CHAIN TRANSFER AND TACTICITY IN FREE RADICAL POLYMERIZATION

In this study, the free radical polymerization of methyl methacrylate (MMA) and N-Isopropylacrylamide (NIPAM) is investigated by using Density Funtional Theory (DFT).

In the first part, the role of thiophenols as chain transfer agents in the polymerization of methyl methacrylate (MMA) is investigated. In many applications, methyl methacrylate is an excellent substitute for glass and it has good mechanical properties. Thiophenols act as chain transfer agents for controlling the molecular weights, thereby the physical properties of some common acrylates such as methyl methacrylate. The correlation between the calculated trend of the chain transfer constants and the experimental results has been reproduced with the MPWB1K/6-311+G(3df,2p) methodolgy.

In the second part of this study the solvent effect on the tacticity of the free radical polymerization of N-Isopropylacrylamide is investigated. Tacticity strongly influences the solution property of Poly(N-Isopropylacrylamide) (PNIPAM). This polymer is a temperature-responsive polymer and called intelligent polymer. It undergoes a reversible phase transition at its lower critical solution temperature (LCST) which is around the body temperature. So, it is used in many areas like drug release. The effect of methanol as a solvent in the polymerization rate and the tacticity of PNIPAM is studied by density functional theory (DFT).

ÖZET

SERBEST RADİKAL POLİMERİZASYONUNDA YAYILMA, ZİNCİR TRANSFERİ VE TAKTİSİTENİN MODELLENMESİ

Bu çalışmada metil metakrilat (MMA) ve N-İzopropilakrilamidin (NIPAM) serbest radikal polimerizasyonları Yoğunluk Fonksiyonları Teorisi (DFT) ile incelenmiştir.

Birinci kısımda, metil metakrilatın polimerizasyonunda tiyofenollerin zincir transferi yapmaları incelendi. Metil metakrilatın iyi mekanik özellikleri vardır ve birçok uygulamada camın yerini alır. Tiyofenoller zincir transferi yaparak metil metakrilat gibi bazı akrilatların moleküler ağırlıklarının, dolayısıyla da fiziksel özelliklerinin kontrol edilmesini sağlarlar. MPWB1K/6-311+(3df,2p) yöntemiyle hesaplanmış olan zincir transfer sabitlerinin eğilimi deneysel sonuçlarla uyumluluk göstermiştir.

Bu çalışmanın ikinci kısımda N-izopropilakrilamidin polimerizasyonunda çözücünün taktisiteye etkisi incelenmiştir. Taktisite poli(N-izopropilakrilamid)in çözelti özelliklerini oldukça etkiler. Isıya duyarlı olan bu polimer, akıllı polimer olarak adlandırılır. Vücut sıcaklığı civarındaki kritik çözelti sıcaklığında (LCST) tersinir faz geçişine uğrar. Bu nedenle ilaç salınımı gibi birçok alanda kullanılmaktadır. Çözücü olarak metanol ün PNIPAM ın polimerizasyon hızına ve taktisitesine etkisi yoğunluk fonksiyonları teorisi (DFT) ile çalışılmıştır.

TABLE OF CONTENTS

LIST OF FIGURES

LIST OF TABLES

LIST OF SYMBOLS/ABBREVIATIONS

$E^{‡}$	Electronic activation energy
E_c^{VWN}	Vosko-Wilk-Nusair correlation functional
E_x^{exact}	Exact exchange energy
$E_c[\rho]$	Correlation energy
$E_x[\rho]$	Exchange energy
$E_{\sigma\sigma^*}$	Non-covalent contributions to the energy
ΔE_x^{B88}	Becke's gradient correction
ΔE_0	Relative electronic energy at 0 K
ΔE_{0+ZPE}	Sum of the change in electronic energy and zero point energy at 0 K
ΔE_{298}	Relative electronic energy at 298 K
$G^{‡}$	Gibbs free energy of activation
ΔG_{298}	Relative Gibbs free energy at 298 K
ΔH_{298}	Relative enthalpy at 298 K
ΔH_{rxn}	Heat of reaction as electronic energy
$J[\rho]$	Coulomb energy
ΔS_{298}	Relative entropy at 298 K
$T[\rho]$	Kinetic energy of interacting electrons
$T_s[\rho]$	Kinetic energy of non-interacting electrons
U_x^{σ}	Exchange energy density
$V_{ee}[\rho]$	Interelectronic interaction energy
V_{KS}	Kohn-Sham potential
$v(r)$	External potential
$\rho(r)$	Electron density
ψi	Kohn-Sham orbitals
B3LYP	Becke-3-parameter Lee-Yang-Parr functional
B88	Becke 88 Exchange Functional
DFT	Density functional theory
HF	Hartree-Fock theory
LDA	Local density approximation

M05-2X	Minnesota 2005 hybrid with doubled portion of HF exchange
MPWB1K	Modified Perdew-Wang-Becke 1 Parameter Method for Kinetics

k_i	Rate constant of initiation
k_p	Rate constant of propagation
k_t	Rate constant of termination
k_{tr}	Rate constant of chain transfer

1. INTRODUCTION

1.1. Free Radical Polymerization

As a synthetic process free radical polymerization has enabled the production of materials that have enriched the lives of millions of people on a daily basis [1].

The polymerization of unsaturated monomers typically involves a chain reaction. In a typical chain polymerization, one act of initiation may lead to the polymerization of thousands of monomer molecules [2].

Free radical polymerization proceeds via a chain mechanism, which basically consists of four types of reactions involving free radicals [1] :

(1) Initiation: radical generation from nonradical species
(2) Propagation: radical addition to a substituted alkene
(3) Chain transfer: atom transfer and atom abstraction reactions
(4) Termination: radical-radical recombination or disproportionation

The initiation step is considered to proceed via two reactions.In the first step, free radicals are generated by thermal or photochemical homolytic cleavage of covalent bonds of an initiator molecule *I*

$$I \xrightarrow{k_d} 2R\bullet \tag{1.1}$$

where k_d is the rate constant for dissociation. In the second part of the initiation newly formed radical species attack to the first monomer molecule to produce the chain initiating species $M_1\bullet$

$$R_1\bullet + M \xrightarrow{k_i} M_1\bullet \tag{1.2}$$

where M represents a monomer molecule and k_i is the rate constant for the initiation step (Eq. 1.2). This process goes on by successive additions of radicals and monomers by a propagation step, which is the main reaction of polymerization. Each addition forms a new radical which resembles the previous one, but is larger by one monomer unit. The general representation for the propagation step is

$$M_n\bullet + M \xrightarrow{k_p} M_{n+1}\bullet \tag{1.3}$$

where k_p is the rate constant for propagation. The propagation step takes place very rapidly and the propagation rate constant is affected by polarity, resonance, medium and steric factors.

In the chain transfer step, activity of the radical center is transferred to another molecule which is a chain transfer agent (*T*). A dead polymer and another radical is formed. By this way, the molecular weight of the growing chain can be controlled. A representative mechanism for the chain transfer is

$$P_i\bullet + T \xrightarrow{k_{tr}} P_i + T\bullet \tag{1.4}$$

where k_{tr} is the rate constant for chain transfer. Chain transfer can occur to all substances present in a polymerization system.

The polymerization reaction ends up by the combination (coupling) or disproportionation of the two radicals in a termination step. Termination reaction leads to the deactivation of the propagating radical chain ends. In combination, two radicals react with each other,

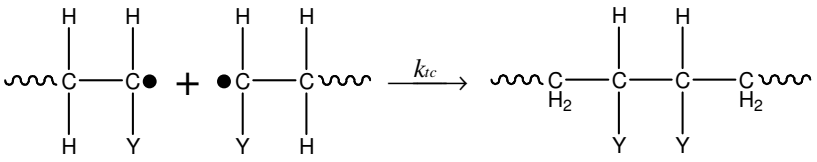

(1.5)

and a hydrogen radical that is beta to a radical center is transferred to another radical center by disproportionation

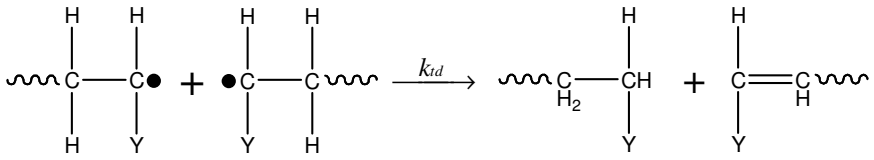

(1.6)

where k_{tc} is the rate constant for termination by combination and k_{td} by disproportionation. These two reactions can be depicted by

$$M_n\bullet + M_m\bullet \xrightarrow{k_{tc}} M_{n+m} \tag{1.7}$$

$$M_n\bullet + M_m\bullet \xrightarrow{k_{td}} M_n + M_m \tag{1.8}$$

or in general terms by

$$M_n\bullet + M_m\bullet \xrightarrow{k_t} \text{dead polymer} \tag{1.9}$$

where the termination rate constant is expressed by the sum of rate constants of the two reactions as

$$k_t = k_{tc} + k_{td} \tag{1.10}$$

The mode of termination affects the nature of end groups, thereby the final properties of the formed polymer. So, the termination reaction is of great importance since it influences the molecular weight distribution or some of the properties of the product in radical polymerization reactions.

1.2. Free Radical Polymerization Kinetics

For the production of polymeric products for a wide range of applications, understanding of free radical polymerization kinetics is very important.

The rate of generation of free radicals that initiate the polymerization can be expressed as

$$v_i = -2f\frac{d[I]}{dt} = 2fk_d[I] \tag{1.11}$$

where f is the initiator efficiency, k_d is the rate coefficient of the initiator decomposition, and [I] is the initiator concentration. Not all generated free radicals initiate polymer growth. They may react in alternative ways before reacting with a monomer unit. So, an efficiency of zero corresponds to no initiation taking place, whereas f = 1 indicates that every generated free radical initiates the polymerization [1].

The process of termination is a bimolecular reaction and the rate expression can be written as follows

$$v_t = 2k_t[M\cdot]^2 \tag{1.12}$$

where k_t is the rate constant for termination and [M·] is the radical concentration. The rate constant $2k_t$ is actually (k_{tc} + k_{td}).

The rate of propagation, and therefore the rate of polymerization is

$$v_p = k_p[M\cdot][M] \tag{1.13}$$

where k_p is the rate constant for propagation, [M] is the monomer concentration.

Radical concentrations are difficult to measure so it is desirable to eliminate [M·] from equation 1.13. For this purpose, the steady-state assumption is made that the

concentration of radicals increases initially, but almost instantaneously reaches a constant, steady-state value. The rate of change of the concentration of radicals quickly becomes and remains zero during the polymerization. So, the rate of initiation υ_i and rate of termination υ_t are equal to each other [3].

$$\upsilon_i = \upsilon_t \tag{1.14}$$

$$2fk_d[I] = 2k_t[M\cdot]^2 \tag{1.15}$$

$$[M\cdot] = \left(\frac{fk_d[I]}{k_t}\right)^{1/2} \tag{1.16}$$

Thus, the rate of propagation, υ_p, may be given as

$$\upsilon_p = k_p[M]\left(\frac{fk_d[I]}{k_t}\right)^{1/2} \tag{1.17}$$

where [M·] in the equation 1.13 is replaced by the expression in equation 1.16. Then, the final expression for the rate of polymerization, R_p is

$$R_p = -\frac{d[M]}{dt} = k_p\left(f\frac{k_d}{k_t}\right)^{1/2}[M][I]^{1/2} \tag{1.18}$$

where k_p stands for the propagation rate constant. In the derivation of polymerization rate, the propagation (k_p) and the termination (k_t) rate coefficients are assumed to be chain length and conversion independent [4, 5].

2. METHODOLOGY

2.1. Reaction Rate Calculations

For the calculation of reaction rate constants, *Activated Complex Theory*, which is also called *Transition State Theory*, is used by the help of statistical thermodynamics [6].

Transition state theory pictures a reaction between A and B as proceeding through the formation of an activated complex, $C^{\neq}$, in a rapid pre-equilibrium and the activated complex falls apart by a unimolecular decay into products, P, which can be shown as

$$A + B \rightleftharpoons C^{\neq} \rightarrow P$$

The equilibrium constant for this reaction can be given as

$$K^{\neq} = \frac{N_A q_{c^{\neq}}^{\theta}}{q_A^{\theta} q_B^{\theta}} \, e^{-\Delta E_0 / RT} \tag{2.1}$$

where the q_J^{θ} are the standard molar partition functions and ΔE_0 is the difference in molecular energies of the activated complex and the reactants (with inclusion of zero point vibrational energies) which is expressed by the equation

$$\Delta E_0 \; = \; E_0(C^{\neq}) - \; E_0(A) - E_0(B) \tag{2.2}$$

The partition function of the complex can be denoted as

$$q_{c^{\neq}} \approx \frac{kT}{h\upsilon} \, \bar{q}_{c^{\neq}} \tag{2.3}$$

where $\bar{q}_{C^{\neq}}$ is the partition function for all the other modes of the complex.

The constant $K^{\neq}$ is therefore

$$K^{\neq} = \frac{kT}{h\upsilon}\,\overline{K}^{\neq} \tag{2.4}$$

$$\overline{K}^{\neq} = \frac{N_A \overline{q}^{\theta}_{C^{\neq}}}{q^{\theta}_A q^{\theta}_B}\, e^{-\Delta E_0/RT} \tag{2.5}$$

$$k_2 = k^{\neq}\frac{RT}{P^{\theta}}\,K^{\neq} = \kappa\,\upsilon\,\frac{kT}{h\upsilon}\frac{RT}{P^{\theta}}\overline{K}^{\neq} \tag{2.6}$$

After writing

$$\overline{K}_c^{\neq} = \left(\frac{RT}{p^{\theta}}\right)\overline{K}^{\neq} \tag{2.7}$$

the *Eyring equation* is obtained:

$$k_2 = \kappa\,\frac{kT}{h}\,\overline{K}_c^{\neq} \tag{2.8}$$

Provided that $\overline{K}_c^{\neq}$ is the equilibrium constant (despite one mode of $C^{\neq}$ having been discarded), it can be expressed in terms of *Gibbs energy of activation*, $\Delta G^{\neq}$, by the equation

$$\Delta G^{\neq} = -RT\ln\overline{K}^{\neq} \tag{2.9}$$

Then, the rate constant becomes

$$k_2 = \kappa\frac{kT}{h}\frac{RT}{P^{\theta}}e^{-\Delta G^{\neq}/RT} \tag{2.10}$$

where k represents Boltzman's constant, T is the temperature, h is the Planck's constant, $\Delta G^{\neq}$ represents the molecular Gibbs free energy difference between the activated complex and the reactants (with inclusion of zero point vibrational energies), R is the universal gas constant, κ is the transmission coefficient, and P^{θ} is the standard pressure 10^5 Pa (1 bar).

Chain transfer constant, C_{tr}, is a measure of the reactivity of a chain transfer agent and can be computed as follows:

$$C_{tr} = \frac{k_{tr}}{k_p} \tag{2.11}$$

where k_{tr} is the chain transfer rate constant and k_p is the propagation rate constant. The higher C_{tr}, the lower the concentration of the chain transfer agent required for a particular molecular weight reduction [7].

2.2. Density Functional Theory

The Density Functional Theory (DFT) [8] is based on the Kohn-Hohenberg theorems proposed in 1964 [9, 10]. It is a quantum mechanical approach to the electronic nature of atoms and molecules. Kohn-Hohenberg theorems state that all the ground-state properties of a system are functions of the charge density.

The first theorem of DFT states that the electron density $\rho(r)$ determines the external potential $v(r)$, i. e. the potential due to the nuclei. The second theorem introduces the variational principle. Hence, the electron density can be computed variationally and the position of nuclei, energy, wave function and other related parameters can be calculated [8, 11].

The electron density is defined as:

$$\rho(x) = N \int \ldots \int \left|\Psi(x_1, x_2, \ldots x_n)\right|^2 dx_1 dx_2 \ldots dx_n \tag{2.12}$$

where x represents both spin and spatial coordinates of electrons.

The electronic energy can be expressed as a functional of the electron density:

$$E[\rho] = \int v(r)\rho(r)dr + T[\rho] + V_{ee}[\rho] \tag{2.13}$$

where $T[\rho]$ is the kinetic energy of the interacting electrons and $V_{ee}[\rho]$ is the interelectronic interaction energy. The electronic energy may be rewritten as

$$E[\rho] = \int v(r)\rho(r)dr + T_s[\rho] + J[\rho] + E_{xc}[\rho] \tag{2.14}$$

with $J[\rho]$ being the coulomb energy, $T_s[\rho]$ being the kinetic energy of the non-interacting electrons and $E_{xc}[\rho]$ being the exchange-correlation energy functional. The exchange-correlation functional is expressed as the sum of an exchange functional $E_x[\rho]$ and a correlation functional $E_c[\rho]$, although it contains also a kinetic energy term arising from the kinetic energy difference between the interacting and non-interacting electron systems. The kinetic energy term, being the measure of the freedom, and exchange-correlation energy, describing the change of opposite spin electrons (defining extra freedom to an electron), are the favorable energy contributions. The Coulomb energy term describes the unfavorable electron-electron repulsion energy and therefore disfavors the total electronic energy [12].

In Kohn-Sham density functional theory, a reference system of independent non-interacting electrons in a common, one-body potential V_{KS} yielding the same density as the real fully-interacting system is considered. More specifically, a set of independent reference orbitals ψ_i satisfying the following independent particle Schrödinger equation are imagined.

$$\left[-\frac{1}{2}\nabla^2 + V_{KS}\right]\psi_i = \varepsilon_i\psi_i \tag{2.15}$$

with the one-body potential V_{KS} defined as

$$V_{KS} = v(r) + \frac{\partial J[\rho]}{\partial \rho(r)} + \frac{\partial E_{xc}[\rho]}{\partial \rho(r)} \tag{2.16}$$

$$V_{KS} = v(r) + \frac{\rho(r')}{|r - r'|}dr' + v_{xc}(r) \tag{2.17}$$

where $v_{xc}(r)$ is the exchange-correlation potential. The independent orbitals ψ_i are known as Kohn-Sham orbitals and give the exact density by

$$\rho(r) = \sum_{i}^{N} |\psi_i|^2 \tag{2.18}$$

if the exact form of the exchange-correlation functional is known. However, the exact form of this functional is not known and approximate forms are developed starting with the local density approximation (LDA). This approximation gives the energy of a uniform electron gas, i. e. a large number of electrons uniformly spread out in a cube accompanied with a uniform distribution of the positive charge to make the system neutral. The energy expression is

$$E[\rho] = T_s[\rho] + \int \rho(r) v(r) dr + J[\rho] + E_{xc}[\rho] + E_b \tag{2.19}$$

where E_b is the electrostatic energy of the positive background. Since the positive charge density is the negative of the electron density due to uniform distribution of particles, the energy expression is reduced to

$$E[\rho] = T_s[\rho] + E_{xc}[\rho] \tag{2.20}$$

$$E[\rho] = T_s[\rho] + E_x[\rho] + E_c[\rho] \tag{2.21}$$

The kinetic energy functional can be written as

$$T_s[\rho] = C_F \int \rho(r)^{5/3} dr \tag{2.22}$$

where C_F is a constant equal to 2.8712. The exchange functional is given by

$$E_x[\rho] = -C_x \int \rho(r)^{4/3} dr \tag{2.23}$$

with C_x being a constant equal to 0.7386. The correlation energy, $E_c[\rho]$, for a homogeneous electron gas comes from the parametrization of the results of a set of quantum Monte Carlo calculations.

The LDA method underestimates the exchange energy by about 10 per cent and does not have the correct asymptotic behavior. The exact asymptotic behavior of the exchange energy density of any finite many-electron system is given by

$$\lim_{x\to\infty} U_x^{\sigma} = -\frac{1}{r} \tag{2.24}$$

U_x^{σ} being related to $E_x[\rho]$ by

$$E_x[\rho] = \frac{1}{2}\sum_{\sigma}\int \rho_{\sigma} U_x^{\sigma} dr \tag{2.25}$$

A gradient-corrected functional is proposed by Becke

$$E_x = E_x^{LDA} - \beta\sum_{\sigma}\int \rho_{\sigma}^{4/3} \frac{x_{\sigma}^2}{1+6\beta x_{\sigma}\sinh^{-1} x_{\sigma}} dr \tag{2.26}$$

where σ denotes the electron spin, $x_{\sigma} = \dfrac{|\nabla\rho_{\sigma}|}{\rho_{\sigma}^{4/3}}$ and β is an empirical constant (β=0.0042). This functional is known as Becke88 (B88) functional [9].

The adiabatic connection formula connects the non-interacting Kohn-Sham reference system (λ=0) to the fully-interacting real system (λ=1) and is given by

$$E_{xc} = \int_0^1 U_{xc}^{\lambda} d\lambda \tag{2.27}$$

where λ is the interelectronic coupling-strength parameter and U_{xc}^{λ} is the potential energy of exchange-correlation at intermediate coupling strength. The adiabatic connection formula can be approximated by

$$E_{xc} = \frac{1}{2} E_x^{exact} + \frac{1}{2} U_{xc}^{LDA} \tag{2.28}$$

since $U_{xc}^{0} = E_x^{exact}$, the exact exchange energy of the Slater determinant of the Kohn-Sham orbitals, and $U_{xc}^{1} = U_{xc}^{LDA}$ [10].

The closed shell Lee-Yang-Parr (LYP) correlation functional [13] is given by

$$E_c = -a \int \frac{1}{1 + d\rho^{-1/3}} \left\{ \rho + b\rho^{-2/3} \left[C_F \rho^{5/3} - 2t_w + (\frac{1}{9} t_w + \frac{1}{18} \nabla^2 \rho) \right] e^{-c\rho^{-1/3}} \right\} dr \tag{2.29}$$

where

$$t_w = \frac{1}{8} \frac{|\nabla \rho(r)|^2}{\rho(r)} - \frac{1}{8} \nabla^2 \rho \tag{2.30}$$

The mixing of LDA, B88, E_x^{exact} and the gradient-corrected correlation functionals to give the hybrid functionals [14] involves three parameters.

$$E_{xc} = E_{xc}^{LDA} + a_0 \left(E_x^{exact} - E_x^{LDA} \right) + a_x \Delta E_x^{B88} + a_c \Delta E_c^{non-local} \tag{2.31}$$

where ΔE_x^{B88} is the Becke's gradient correction to the exchange functional. In the B3LYP functional, the gradient-correction ($\Delta E_c^{non-local}$) to the correlation functional is included in LYP. However, LYP contains also a local correlation term which must be subtracted to yield the correction term only.

$$\Delta E_c^{non-local} = E_c^{LYP} - E_c^{VWN} \tag{2.32}$$

where E_c^{VWN} is the Vosko-Wilk-Nusair correlation functional, a parametrized form of the LDA correlation energy based on Monte Carlo calculations. The empirical coefficients are a_0=0.20, a_x=0.72 and a_c=0.81 [15].

2.3. Continuum Solvation Models

Continuum solvation models are the most efficient way to include condensed-phase effects into quantum mechanical calculations [16]. Advantage of these models is that they decrease the number of the degrees of freedom of the system by describing them in a continuous way, usually by means of a distribution function [17, 18]. In continuum solvation models, the solvent is represented as a polarizable medium characterized by its static dielectric constant ε and the solute is embedded in a cavity surrounded by this dielectric medium. The total solvation free energy is defined as

$$\Delta G_{solvation} = \Delta G_{cavity} + \Delta G_{dispersion} + \Delta G_{electrostatic} + \Delta G_{repulsion} \quad (2.33)$$

where ΔG_{cavity} is the energetic cost of placing the solute in the medium. Dispersion interactions between solvent and solute are expressed as $\Delta G_{d;spersion}$ which add stabilization to solvation free energy. $\Delta G_{electrostatic}$ is the electrostatic component of the solute-solvent interaction energy. $\Delta G_{repulsion}$ is the exchange solute-solvent interactons not included in the cavitation energy.

The central problem of continuum solvent models is the electrostatic problem described by the general Poisson equation:

$$-\vec{\nabla}\left[\varepsilon(\vec{r})\nabla\vec{V}(\vec{r})\right] = 4\pi\rho_M(\vec{r})$$

simplified to

$$-\nabla^2 V(\vec{r}) = 4\pi\rho_M(\vec{r}) \text{ within } C \quad (2.34)$$

$$-\varepsilon\nabla^2 V(\vec{r}) = 0 \text{ outside } C \quad (2.35)$$

where C is the portion of space occupied by cavity, ε is dielectric function, V is the sum of electrostatic potential V_M generated by the charge distribution ρ_M and the reaction potential V_R generated by the polarization of the dielectric medium:

$$V(\vec{r}) = V_M(\vec{r}) + V_R(\vec{r}) \tag{2.36}$$

Polarizable Continuum Model (PCM) belongs to the class of polarizable continuum solvation models [19]. In PCM, the solute is embedded in a cavity defined by a set of spheres centered on atoms (sometimes only on heavy atoms), having radii defined by the van der Waals radius of the atoms multiplied by a predefined factor (usually 1.2). The cavity surface is then subdivided into small domains (called tesserae), where the polarization charges are placed. There are three different approaches to carry out PCM calculations. The original method is called Dielectric PCM (D-PCM), the second model is the Conductor-like PCM (C-PCM) [20] in which the surrounding medium is modeled as a conductor instead of a dielectric, and the third one is an implementation whereby the PCM equations are recast in an integral equation formalism (IEF-PCM).

3. AIM OF THE STUDY

This study is composed of two parts which are mainly about the free radical polymerization of different unsaturated compounds.

In the first part, the propagation and the chain transfer reactions in the free radical polymerization of methyl methacrylate (MMA) are investigated. The kinetics of these reactions are examined by using Density Functional Theory (DFT) and compared with the experimental findings.

The aim of the second part is to investigate the effect of methanol as a solvent on the tacticity and the propagation step of free radical polymerization of n-isopropyl acrylamide (NIPAM) by using quantum mechanical tools.

4. ROLE OF THIOPHENOLS IN THE FREE RADICAL POLYMERIZATION OF METHYL METHACRYLATE

4.1. Introduction

Conventional free radical polymerization is a very important commercial process for preparing high molecular weight polymers. However, it has a lack of control over some of the key elements in macromolecular systems, such as molecular weight, polydispersity, end functionality, chain architecture and composition [21]. So, Controlled/Living Radical Polymerization (CLRP) is a subject of increasing interest in polymer science. CLRP has enabled scientist to develop well-defined polymers with precisely controlled structural parameters and molecular weights.

CLRPs can be listed as the following:

- Nitroxide mediated polymerization (NMP)
- Atom transfer radical polymerization (ATRP)
- Degenerative transfer (DT)
  - i. Reversible addition-fragmentation chain transfer (RAFT) process
  - ii. Macromolecular design via interchange of xanthates (MADIX)
  - iii. (Reversible) Iodine transfer polymerization [(R)ITP]
  - iv. Initiator-transfer agent-terminator (Iniferter) process

Chain Transfer Methods as traditional ways of controlling free radical polymerization can be listed as

- Catalytic Chain Transfer Process (CCT)
- Addition of chain transfer agents to reaction medium

In NMP, the covalent C-ON bond is cleaved upon heating to generate the growing carbon radical species along with the stable aminoxyl or nitroxyl radical. During the polymerization, growing polymer chain end is reversibly capped with the stable counterpart to induce controlled propagation at almost the same rate for each polymer chain [22]. NMP has an advantage over other control methods in that it does not require

addition of a metal complex and this leads to greater functional group tolerance and easier purification. So, there is no contamination by metal ions [24].

In ATRP, the carbon-halogen (C-X) bond is homolytically cleaved by the oxidation of the metal center. The generated carbon radical species induces addition to C=C double bond and a new C-X bond is formed by the reduction of the oxidized metal center. The metal center may include various transition metals such as Ru, Cu, Fe, Ni, Pd, Rh, Mo, Re, etc. The molecular weight control is achieved by the fast reversible activation of the C-X dormant species by the one-electron redox reaction of the metal center [22].

As one of the most popular controlled/living radical polymerization (CLRP) method, RAFT has some advantages over the competing methods. It has a wide range of functionality in monomer and solvent. It is applicable to various types of monomers in a vast range of reaction conditions [21]. RAFT process requires the presence of a monomer, a conventional radical initiator, and a chain transfer agent (CTA) in the reaction medium. The simplified mechanism involves a series of reversible addition-fragmentation chain transfer steps between the CTA and a radical, as well as initiation, propagation, and termination steps. The exchange reaction and propagation process repeat themselves many times so that every chain has a similar chance to grow [24].

MADIX and RAFT processes are identical and they differ in the nature of the chain transfer agents (CTA) used: in RAFT, there is Z-C(=S)-S-R type of CTAs in general whereas MADIX refers to xanthates (R'-O-C(=S)-S-R) exclusively [21].

(Reversible) iodine transfer polymerization ((R)ITP) is another degenerative transfer method in which the polymerization starts with I_2 and a conventional radical initiator, leading to *in situ* generation of transfer agent R-I or P-I (where R is the primary radical from initiator and P is polymer) [25].

Iniferters are initiators, which have very high reactivities for the chain transfer reaction to the initiators and/or primary radical termination [26]. They act as initiators, transfer agent, and terminator in controlled free radical iniferter polymerizations.

Catalytic chain transfer (CCT) agents also have a control on the molecular weight of polymers. Substituted cobalt porphyrins or benzoporphyrins have been shown to provide dramatic reductions in the molecular weight of the methacrylate polymers during radical polymerization with little to no reduction in the overall yield of polymer [27]. Catalytic mode of action and high transfer constant of the cobalt complex, and obtaining polymers with C=C end group make this method preferable for molecular weight control [1].

The classical method of controlling molecular weights is the addition of chain transfer agents to the polymerization medium. For many industrially important systems, a chain transfer agent is added to the polymerization composition in order to lower the polymer molecular weight [28]. A growing macro radical abstracts a hydrogen atom from the chain transfer agent giving a terminated polymer chain and a new initiating radical, which adds to the monomer giving a new propagating species.

The decrease of the molecular weight by the addition of a chain transfer agent is quantitatively given by the Mayo equation [29], which expresses the reciprocal of the polymerization degree (D_{Pn}) as a function of the rate of the chain growth and the chain stopping,

$$\frac{1}{D_{Pn}} = \frac{1+\alpha}{(D_{Pn})_0} + C_{tr}\frac{[CTA]}{[M]} \qquad (4.1)$$

In this equation, $(D_{Pn})_0$ is the polymerization degree in the absence of chain transfer agent, [CTA] is the concentration of the chain transfer agent, [M] is the monomer concentration, and α is the fraction of termination by disproportionation [30].

Experimental and theoretical studies on hydrogen and halogen atom transfer reactions have illustrated the structure-reactivity relationship in these reactions as well as the importance of polar effects in the transition states; several theoretical frameworks such as the curve-crossing model of Shaik and Pross have been developed to explain these results [31, 32]. Recently, high level ab initio calculations have been used to understand the hydrogen abstraction by carbon-centered radicals from thiols where a reasonable correlation between the barrier height and the polar effects has been found [33]. Dolbier et

al. have highlighted the importance of transition-state polar effects in hydrogen atom transfer reactions: the rate of reduction of fluoroalkyl radicals by PhSH has shown that PhS-H, a very efficient H atom donor to hydrocarbon radicals, reduced perfluoro-n-alkyl radicals 500 times slower. This result indicates that transition-state polar effects must also play a significant role in such hydrogen atom transfer reactions [34].

In this study, quantum mechanical calculations have been used to model and understand the role of thiophenols as chain transfer agents in the free radical polymerization of methyl methacrylate (MMA). Polymethyl methacrylate (PMMA) has very good mechanical properties and it has better resistance to alkali than polymethyl acrylate due to the shielding presented by the methyl group. It is resistant to many chemicals but soluble in organic solvents such as ketones, chlorinated hydrocarbons, and esters. Optical clarity is the main feature of this plastic. So, it is widely used in contact lenses, camera lenses, watch crystals and aircraft glass [35, 36].

4.2. Methodology

4.2.1. Computational Procedure

Density functional theory was used for all geometry optimizations by using the Gaussian 03 program package [37]. B3LYP/6-31+G(d) methodology was selected as a cost-effective method because it was also used in previous reports to model the free radical propagation reactions [38-43]. Although B3LYP is accurate for geometry optimizations, it is not suitable for obtaining kinetic results [44]. Different hybrid meta GGA functionals, MPWB1K [45] and M05-2X [46], have been used to obtain more realistic kinetic results. A recent study on hybrid meta DFT methods has shown that MPWB1K can be used with confidence for a combination of thermochemistry, thermochemical kinetics, hydrogen bonding, and weak interactions, especially for thermochemical kinetics and noncovalent interactions [45]. M05-2X is a hybrid meta exchange-correlation functional that was designed for very general purposes such as kinetics, thermochemistry of main group elements, noncovalent interactions, ionization potentials, and activation energies [46]. For the activation energy barriers, it was found that M05-2X is less accurate than BB1K,

PWB6K, MPWB1K, MPW1K, BMK, for H-abstraction reactions but more accurate than B3LYP and other functionals [46].

The transition structures for the addition, hydrogen abstraction and chlorine abstraction reactions have a very low vibrational frequency, corresponding to the internal rotation of the incoming radical about the forming bond. Recent studies of radical addition [38, 40, 41, 47-49] and hydrogen abstraction reactions [50-52] have been modeled by using the 1D-HR approach. In this study a mixed harmonic oscillator/hindered rotor (HO/HR) model, in which all the internal motions except the internal rotations corresponding to bond formation are approximated as independent harmonic oscillators, was used. Tunneling corrections for the abstraction of hydrogen have been used in modeling since the abstracted hydrogen atom is light and its wavelength is large compared with the barrier width, thereby enabling it to 'tunnel' through the barrier. Hybrid DFT methods such as MPW1K and B3LYP have been used to obtain reasonable estimates of the tunneling coefficients -to within a factor of 2–3 [53]. In recent studies both Wigner [54] and Eckart [55] methodologies have been used successfully for hydrogen abstraction reactions [38, 56].

To calculate the bond dissociation energies of the chain transfer agents we have made use of isodesmic reactions which conserve the number of each bond type on either side of the reaction resulting in significant improvements in calculated reaction enthalpies due to the cancellation of systematic calculation errors [57].

For the reaction

$$\text{4-X-PhS-H} \rightarrow \text{4-X-PhS}\cdot + \text{H}\cdot \qquad (4.2)$$

the isodesmic reaction

$$\text{4-X-PhS-H} + \text{HS}\cdot \rightarrow \text{4-X-PhS}\cdot + \text{H}_2\text{S} \qquad (4.3)$$

has been utilized to determine the bond dissociation energy of 4-X-PhS-H as

$$\text{BDE (4-X-PhS-H)} = \Delta H_{rxn}(4.3) - \Delta_f H^0_{298}(\text{H}_2\text{S}) + \Delta_f H^0_{298}(\text{HS}\cdot) + \Delta_f H^0_{298}(\text{H}\cdot) \qquad (4.4)$$

where $\Delta_f H^0_{298}$ (H_2S) = - 4.94 kcal mol^{-1}, $\Delta_f H^0_{298}$ (HS·) = 34.20 kcal mol^{-1}, $\Delta_f H^0_{298}$ (H) = 52.10 kcal mol^{-1} have been used [58].

In this study, the propagation and chain transfer reactions of methyl methacrylate have been modeled with the B3LYP/6-311+G(3df,2p)//B3LYP/6-31+G(d), MPWB1K/6-311+G(3df,2p)//B3LYP/6-31+G(d) and M05-2X/6-311+G(3df,2p)//B3LYP/6-31+G(d) methodologies. Calculations were carried out at 298.15 K. The effect of a polar environment was taken into account by use of the self-consistent reaction field (SCRF) theory, utilizing the integral equation formalism-polarizable continum (IEF-PCM) model in solution [59-62]. The solvent was taken to be acetonitrile as described experimentally [63]. At each level of theory, free energies of each species in solution were obtained as the sum of the corresponding gas-phase free energy, the calculated free energy of solvation with non-electrostatic effects and a correction term, RT ln(24.46), to take account of the fact that the solvation energy is computed for the passage from 1 mol L^{-1}(g) to 1 mol L^{-1}(soln) [64].

4.3. Results and Discussion

4.3.1. Propagation of MMA

The free radical polymerization of methylmethacrylate is modeled as depicted in Figure 4.1.

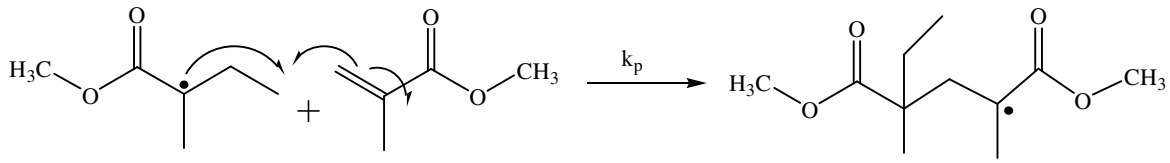

Figure 4.1. Mechanism for the propagation reaction of MMA.

As already known experimentally and demonstrated computationally, the syndiotactic polymer is preferred over the isotactic one [39]. A conformational analysis has been carried out for the syndiotactic propagating radical chain (Figure 4.2). The most stable conformer has been found to be the one with $\tau = 60.12^0$, the gauche addition is

preferred. The global minimum of this transition structure is stabilized by long range H---O interactions (-O-H_2C–H---O=C-). The propagation rate constant k_p for the lowest energy conformer has been considered in the calculation of C_{tr}.

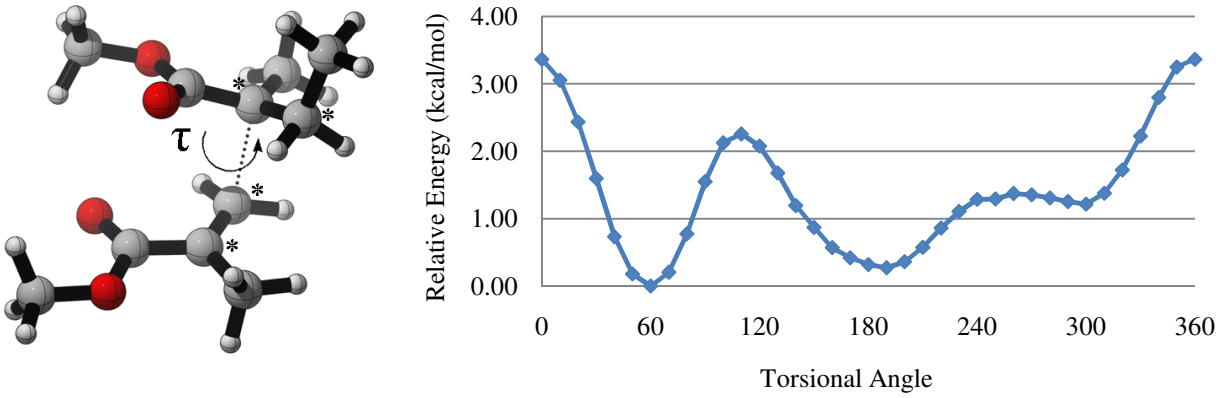

Figure 4.2. Transition state and potential energy scan along τ for the propagation reaction of MMA (B3LYP/6-31+G(d)).

4.3.2. Chain Transfer Reaction in MMA

The addition of thiophenols to the polymerization of methyl methacrylate in organic media is known to reduce considerably the polymer molecular weight without variations in the polymerization rate (Figure 4.3) [63]. The data collected for 4-X-thiophenols has shown that k_{tr} was markedly dependent on the 4-substituent, the higher rate constant was obtained for the thiophenol bearing the strong electron donor amino group.

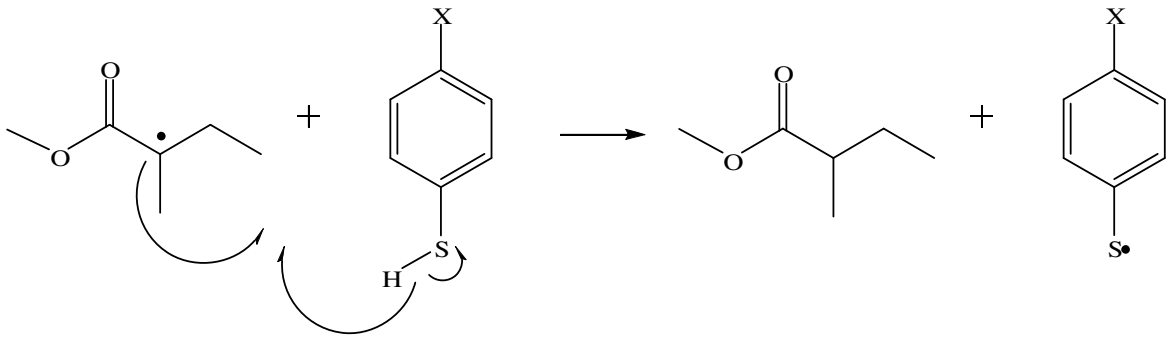

Figure 4.3. Chain transfer reaction between 4-X-thiophenols and MMA (X= Cl, H, CH_3, OCH_3, OH, NH_2)

For the transition states, the potential energy scan along the critical bond (S-H---C·) has been performed for X=H and the global minimum is found to correspond to the dihedral angle C-S---C·-C(C=O) having a value of 96.20^0, all the other transition structures follow this trend (Figure 4.4).

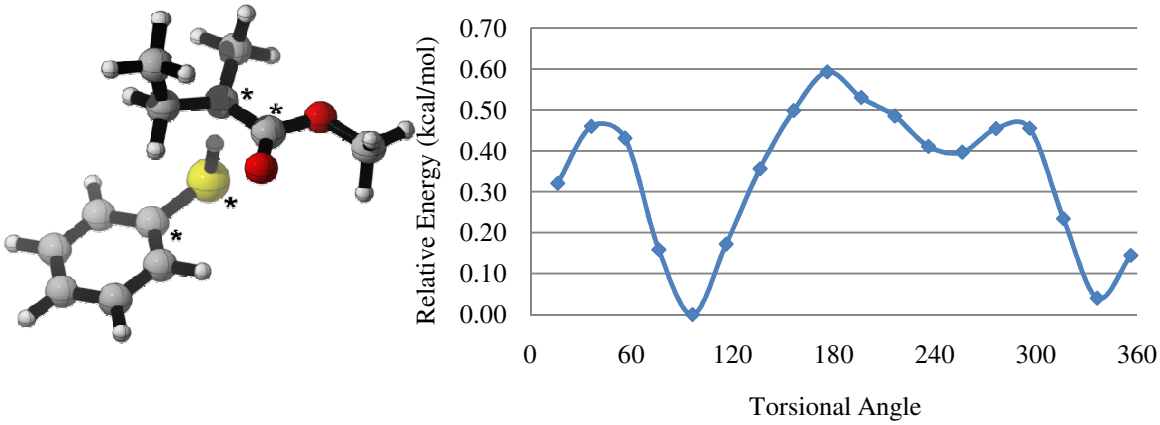

Figure 4.4. Transition state and potential energy scan along the critical bond for the chain transfer reaction (B3LYP/6-31+G(d)).

The lengths of the forming and breaking bonds in the transition states are a consequence of the electronic nature of the substituents at position 4, e.g. the more electron donor the substituent, the shorter is the breaking bond and longer is the forming bond, the earlier is the transition state (Figure 4.5). Also notice that, as the electron-donation capacity of the substituent increases, the difference between the forming and breaking bond distances increases. The greatest difference is observed when the substituent is an amino group, due its higher the electron donation capability (Figure 4.5).

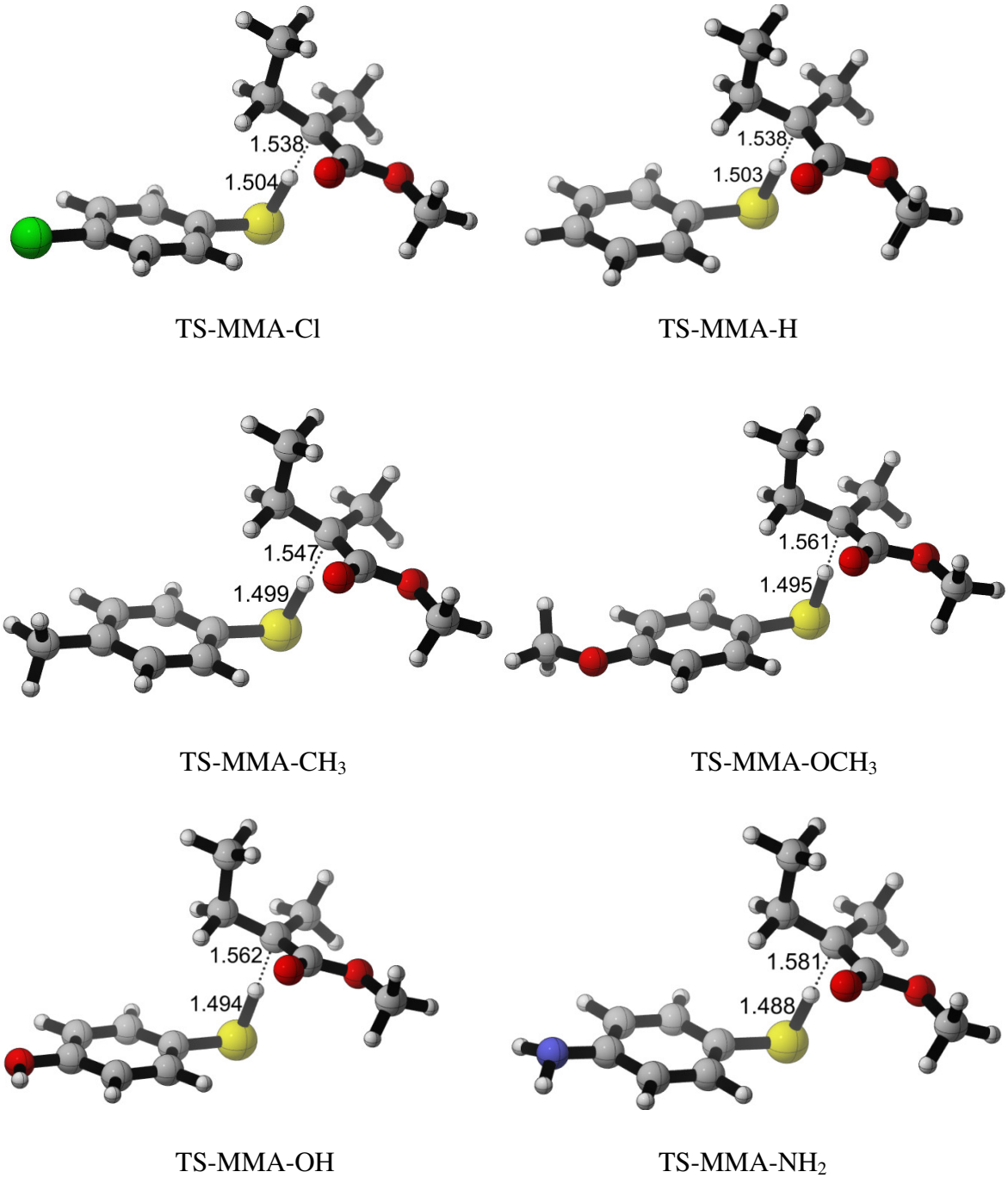

Figure 4.5. Transition states for the chain transfer reactions in the FRP of MMA (B3LYP/6-31+G(d)).

4.3.3. Analysis of the Computational Findings

The hydrogen abstraction by the radical of MMA (MMAR) from 4-X- thiophenols is an exothermic process in which a strong C-H bond is formed and a weak S-H bond is

broken. The BDE of MMA (89.6 kcal mol^{-1}) is higher than the BDEs of the S-H bond dissociation energies (Table 4.1). This is in agreement with a study on hydrogen abstraction from thiols by carbon-centered radicals [33]. The reaction barriers are the lowest for the most electron donor groups: $–OCH_3$, -OH and $–NH_2$. The S-H BDEs of thiols fall into a relatively narrow range despite the wide variation in the properties of the substituents which can be explained in terms of the para location of the substituent insulating the substituent from the breaking S-H bond. To explore the effect of the various descriptors used in the curve-crossing model of Shaik and Pross [31, 32] the reaction barriers have been plotted against the reaction enthalpy, the average singlet-triplet gap of the closed shells reactants and products, the energy for charge transfer between the isolated alkyl and thiyl fragments of the transition structures and the difference in the charges on the alkyl and thiyl fragments of the transition structures. Charge transfer energies (eV) were calculated as the difference in the vertical ionization energy of the donor species and the vertical electron affinity of the acceptor. R^+SR^- refers to charge transfer from the monomer-radical fragment to the thiyl fragment, while R^-SR^+ refers to charge transfer from the thiyl to the monomer radical.

Table 4.1. Forward Barrier ($\Delta H^{\neq}_{fwd}$), Reverse Barrier ($\Delta H^{\neq}_{rev}$), Enthalpy (ΔH), Charge – Transfer Energies (R^+SR^- and R^-SR^+) and NBO Charges (Q) on the Alkyl and Thiyl Fragments in the Transition Structures for $CH_3MMA\cdot + HSPhX \rightarrow CH_3MMAH + \cdot SPhX$ (MPWB1K/6-311+G(3df,2p)//B3LYP/6-31+G(d))

X	$\Delta H^{\neq}_{fwd}$	$\Delta H^{\neq}_{rev}$	ΔH	R^+SR^-	R^-SR^+	Q(alkyl)	Q(thiyl)	BDE
H	6.1	13.7	-7.6	6.92	9.19	-0.046	-0.118	79.4
Cl	5.7	13.8	-8.2	7.32	9.15	-0.041	-0.125	78.8
CH_3	5.6	14.4	-8.8	6.95	8.88	-0.052	-0.111	78.2
OCH_3	5.2	15.9	-10.7	7.00	9.21	-0.054	-0.108	76.2
OH	4.7	15.4	-10.7	7.05	9.46	-0.056	-0.108	76.2
NH_2	4.6	17.6	-13.1	6.89	-	-0.062	-0.098	74.5

Among these descriptors a reasonable correlation between the barrier height and the reaction enthalpy obeying the Evans-Polanyi rule [65] has been determined as displayed in Figure 4.6. In all cases the preferred direction of charge transfer is from the alkyl radical to the thiyl radical (the R^+SR^- configuration is preferred). This finding is confirmed by the lower charge-transfer energies for the R^+SR^- configuration and also by the negative charges

on the thiyl fragment in the transition structure. In general the electron donating groups on the thiyl radical increase the charge-transfer stabilization of the transition state and lower the barrier compared with the non-substitued case (X=H).

These results suggest that polar interactions influence highly the barrier heights in hydrogen abstraction from thiols by CH_3-MMA· .

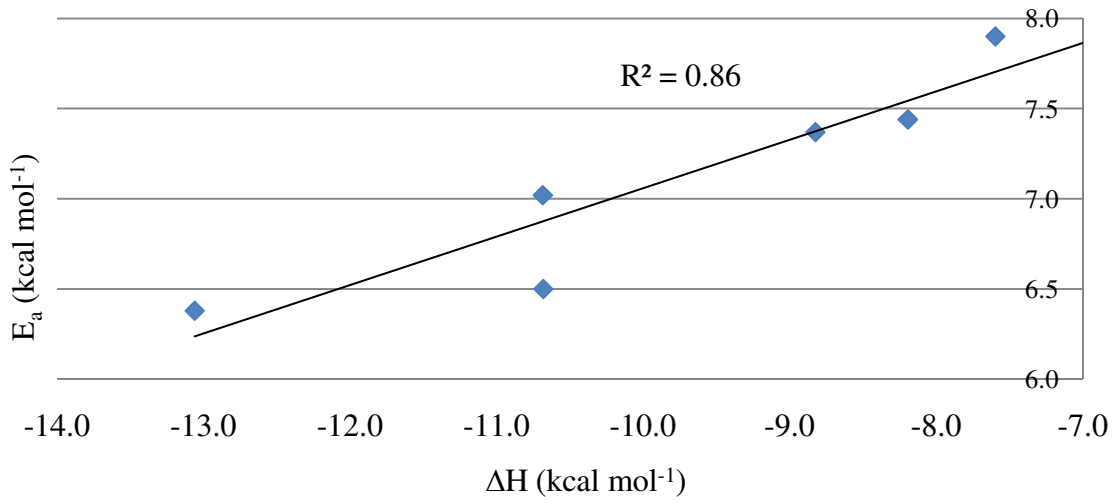

Figure 4.6. Reaction barrier versus reaction enthalpy (MPWB1K/6-311+G(3df,2p)//B3LYP/6-31+G(d)).

4.3.4. Level of Theory Study

The methodology used has been tested and an LOT study has been performed on the chain transfer constant, C_{tr}, for the free radical polymerization of MMA with the MPWB1K, B3LYP, and M05-2X methodologies. The mean unsigned error (MUE) is similar with all methodologies; even though B3LYP yields the highest regression coefficient, the MPWB1K values lie closer to the normalized experimental values (Table 4.2 and Figure 4.7).

Table 4.2. LOT study on the chain transfer rate constants (k_{tr}) of 4-X-thiophenols in the FRP of MMA (298.15K).

X—⟨⟩—SH		k_{tr} exp [63]	k_{tr} Calculated				
X			B3LYP	MPWB1K	M05-2X	MPWB1K-(Solution)*	MPWB1K**
1	Cl	900	2.61E+01	7.34E+01	1.44E+04	4.50E-02	6.07E+02
2	H	1900	1.85E+01	4.81E+01	8.20E+03	7.74E-02	4.19E+02
3	CH_3	4500	2.65E+01	8.75E+01	1.28E+04	1.46E-01	7.01E+02
4	OCH_3	7580	5.56E+01	8.01E+01	1.11E+04	3.47E-01	6.09E+02
5	OH	8900	1.25E+02	3.31E+02	2.89E+04	1.48E+00	2.38E+03
6	NH_2	13100	2.13E+02	4.64E+02	3.74E+04	3.13E+00	3.17E+03
MUE*			1.60	1.48	1.37	8.18	0.98
R^2			0.86	0.77	0.70	0.81	0.76
STDEV			1.78	1.92	0.87	7.78	1.52

* The solvent is acetonitrile.
**Corrected with HIR and Eckart tunneling corrections.
[k_p (B3LYP/6-311+G(3df.2p)//B3LYP/6-31+G(d)) = 4.14E-03 $Lmol^{-1}s^{-1}$;
(MPWB1K/6-311+G(3df,2p)//B3LYP/6-31+G(d)) = 5.87E+00 $Lmol^{-1}s^{-1}$,
(M05-2X/6-311+G(3df,2p)//B3LYP/6-31+G(d)) = 4.50E+03 $Lmol^{-1}s^{-1}$;
(MPWB1K/6-311+G(3df,2p)//B3LYP/6-31+G(d)-acetonitrile) = 1.39E-02 $Lmol^{-1}s^{-1}$].

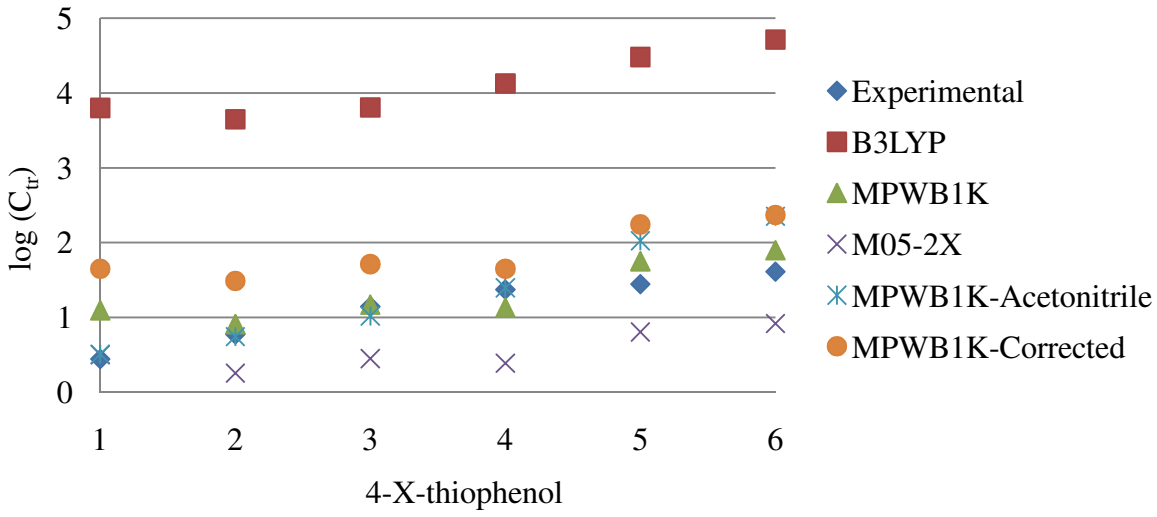

Figure 4.7. log(C_{tr}) versus 4-X-thiophenols in the FRP of MMA (Table 4.2).

In this study, even though accurate predictions of rate constants failed with DFT methodologies as claimed in previous studies on radicals [66-68], reasonable agreement

with the experimental trends has been achieved with all the three methodologies. Among the three methods tested, MPWB1K was found to the best one.

Tunneling corrections have been evaluated with Eckart's methodology. For H transfer reactions these corrections are meaningful since there is no tunneling in the propagation reaction; its neglect in hydrogen transfer leads to a non-canceling error. Tunneling corrections increase the rate constants by approximately three orders of magnitude (Table 4.3). HIR corrections amount to 2.31 for MMA whereas they are between 2 and 3 for the chain transfer reactions of MMA. Overall, HIR corrections are seen to cancel each other in the case of C_{tr} whereas tunneling corrections for H-abstraction reactions increase the magnitude of C_{tr} and the experimental trend is reproduced with tunneling corrected C_{tr} as well.

Table 4.3. Tunneling and HIR corrections for MMA.

X	Tunneling Correction	HIR Correction
Cl	3.40	2.43
H	3.45	2.53
CH_3	3.31	2.42
OCH_3	3.08	2.47
OH	2.98	2.41
NH_2	2.72	2.51
Propagation	-	2.31

The effect of the solvent has been taken into account for the chain transfer constant, C_{tr} for 4-X-thiophenols with the MPWB1K/6-311+G(3df,2p)//B3LYP/6-31+G(d) methodology in acetonitrile. The experimental C_{tr} values are very well matched for the first four 4-X-thiophenols (X= Cl, H, CH_3 and OCH_3) (Figure 4.6); the discrepancy for the last two thiophenols (X=OH and NH_2) can be attributed to the H-bonding capacity of the latter which is not taken into account with the continuum model. Long range interactions between the solvent, CH_3CN and the substituents (OH and NH_2) are expected to take place, explicit solvent molecules must be included in order to mimic the accurate experimental trend.

4.3.5. Hammett Plots

Hammett quantified the effect of substituents on any reaction by defining an empirical electronic parameter σ which is derived from the acidity constants of substituted benzoic acids. Thus the electronic substituent parameter σ_X for any substituent X is defined by

$$\sigma_X = \log\frac{K_X}{K_H} \tag{4.5}$$

where K_X and K_H are the acidity constants for the substituted benzoic acid and benzoic acid, respectively, in water at 25^0C. The σ value of a substituent is a measure of the electron-withdrawing or electron-releasing ability of that substituent compared with H. So, it is possible to analyze substituent effects on the rate or equilibrium constants for other reactions. This is done by plotting the set of rate (or equilibrium) constants for a given reaction against the σ values of the substituents. The resulting correlations are expressed by

$$\sigma_p = \log\frac{k_X}{k_H} \tag{4.6}$$

for rate constants. These two equations are together known as the Hammett equations [69].

In order to examine the substituent effects on reactivity in chain transfer reactions of MMA calculated chain transfer rate constants (k_{tr}) have been plotted against the σ_p parameters [70]. (Table 4.4 and Figure 4.8)

Table 4.4. Hammett substituent constants (σ_p) .

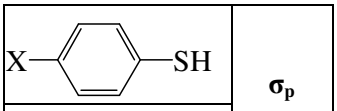 X	σ_p
X	
Cl	0.22
H	0
CH_3	-0.17
OCH_3	-0.28
OH	-0.37
NH_2	-0.63

According to Hammett plots for both experimental and calculated chain transfer rate constants, the rate of chain transfer agents is directly proportional to the electronic strength of the substituents. The σ_p values of 4-X-thiophenols with X being a weak electron donor substituent, cause a slight deviation from linearity. Thus by excluding 4-Cl-thiophenol from the Hammett plots of MMA linear relationships with $R^2 = 0.85$ is obtained. As a result, The role of polar effects in the case of 4-X-thiophenols is confirmed by the strong correlations between the calculated rate constants and Hammett constants.

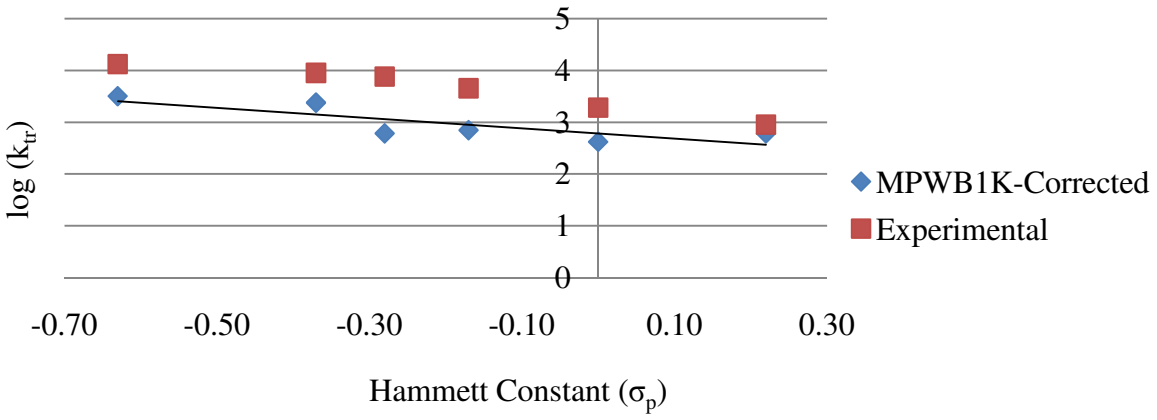

Figure 4.8. Hammett plot for calculated chain transfer rate constant (k_{tr}) (MPWB1K/6-311+G(3df,2p)//B3LYP/6-31+G(d)) values of MMA.

4.4. Conclusions

In this study, the reactivity of 4-X-thiophenols as chain transfer agents in the free radical polymerization of methyl methacrylate has been modeled with quantum chemical tools. The B3LYP/6-311+G(3df,2p)//B3LYP/6-31+G(d), MPWB1K/6-311+G(3df,2p) //B3LYP/6-31+G(d) and M05-2X/6-311+G(3df,2p)//B3LYP/6-31+G(d) methodologies have been tested against the experimental results in order to assess the level of theory. The MPWB1K/6-311+G(3df,2p)//B3LYP/6-31+G(d) methodology is found to reproduce the experimental trend the best. The electron-releasing ability of the 4-X substituent is found to accelerate the chain transfer process. The relationship between the electronic features of the substituent and the rate of chain transfer has been illustrated with Hammett plots. Overall, the models used in this study have proved to be adequate in the rationalization of the FRP kinetics. Similar calculations can be carried out with confidence to predict the characteristics of the chain transfer agent prior to experimental results.

5. SOLVENT EFFECT ON TACTICITY IN THE POLYMERIZATION OF N-ISOPROPYLACRYLAMIDE

5.1. Introduction

5.1.1. Stereocontrol in Free Radical Polymerization

Even though it is hard to control the growing chains, the free radical polymerization is one of the most favorable chemical reactions employed in the industry because it is possible to obtain high molecular weight polymeric materials from a wide variety of vinyl monomers without extensive purification [22]. However, besides the molecular weight, the tacticity of the growing chain should be controlled in the free radical polymerization. Because, tacticity is a mesaure of stereoregularity of a polymer chain and many of the polymer properties such as tensile strength, melting point, and solubility depend on it, tacticity control is an important goal [71]. There are two fundamental approaches for stereochemical control of polymers during free radical polymerization [1]: (1) catalytic control of the propagating chain end using Lewis acids, solvents, and chiral auxiliaries, and (2) use of polymerizations in organized and constrained media.

Tacticity is the relationship between the two adjacent monomer units consisting of meso (m) and racemo (r) diads (Figure 5.1) [22]. An *isotactic* polymer contains only successive meso-diads in the chain and a *syndiotactic* polymer only racemo-diads. If the meso and racemo-diads are appearing alternatingly along the chain, the polymer is called *heterotactic*. Finally, if the R groups on successive stereocenters are randomly distributed, the polymer does not have an order and is called as *atactic* [1, 3].

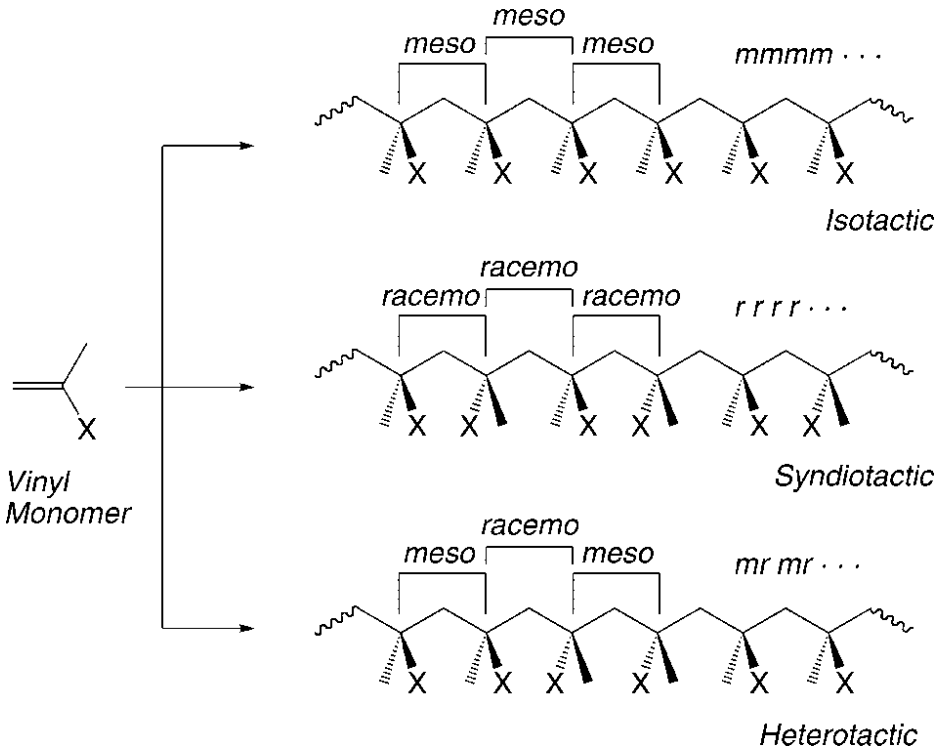

Figure 5.1. Tacticity of vinyl polymers.

5.1.2. N-Isopropylacrylamide (NIPAM)

Recently, N-isopropylacrylamide (NIPAM) (Figure 5.2a) has attracted great attention because its polymer, poly(N-isopropylacrylamide) (PNIPAM) (Figure 5.2b), has a lower critical solution temperature around human body temperature (LCST=32^{0}C) [72]. LCST is the critical temperature where the polymer shows a phase transition because of the alterations in the hydrogen bonding interactions of the amide group. Because the hydrophobic interactions are favored above the critical temperature, the polymer collapses, whereas it is hydrophilic and expands below the LCST [73, 74]. This behaviour makes PNIPAM a good candidate for the synthesis of hydrogels, drug delivery devices, reaction catalysis, and protein folding [74-76].

(a) (b)

Figure 5.2. Structures of (a) NIPAM and (b) PNIPAM.

Tacticity strongly influences the solution property of PNIPAM. It was reported that PNIPAM with isotactic content over 72 % was insoluble in water, whereas atactic one showed a phase transition around 32 ^{0}C. As the syndiotactic content increased from 53 to 71 %, Tc (the cloud point) increased from 33.1 to 35.9 ^{0}C [77]. Several studies have been done in the literature in order to control the stereochemistry of PNIPAM during the free radical polymerization. Hirano et al. showed that the presence of pyridine N-oxide (PNO) induced isotacticity in the radical polymerization of NIPAM [78, 79]. Also, they have found that stereocontrol can be achieved under metal-free conditions by forming hydrogen-bond-assisted complexes with NIPAM and Lewis bases like hexamethylphosphoramide (HMPA) which induced syndiotacticity [80]. Because PNIPAM is a thermo-responsive polymer, not only the hydrogen bond assistance, but also the temperature affects the final properties of the polymer [79, 81]. It was reported that some simple alkyl alcohols such as methanol, *t*-butanol, and 3-methyl-3-pentanol played dual roles in the polymerization system by increasing the formation of syndiotactic specific PNIPAM, and accelerating the polymerization reaction [77].

5.2. Methodology

5.2.1. Computational Procedure

Density Functional Theory (DFT) with Gaussian03 program package was used for all the calculations. Geometry optimizations were done with the B3LYP/6-31+G(d) methodology. For the kinetic calculations, 6-311+G(d,p) basis set was used with B3LYP functional.

In this study, solvation free energy of PNIPAM polymerization was calculated in three ways: (1) By using an implicit solvation model with the conductor-like polarizable continuum model (CPCM) [82] in methanol with Pauling radii [83]. (2) By adding explicit methanol molecules to the structures to see the effect of hydrogen-bond-assistance on the transition structures and solvation free energies. (3) A mixed implicit/explicit solvation model was used. For this purpose, the position of methanol molecules was found explicitly and implicit solvent calculations for this new model were done with the CPCM solvation model.

5.3. Results and Discussion

In this study, propagation reaction of PNIPAM is modeled as shown in Figure 5.3. The structure of the propagating NIPAM radical is considered by replacing the long polymer chain with a radical derived from the attack of $CH_3\cdot$ to NIPAM.

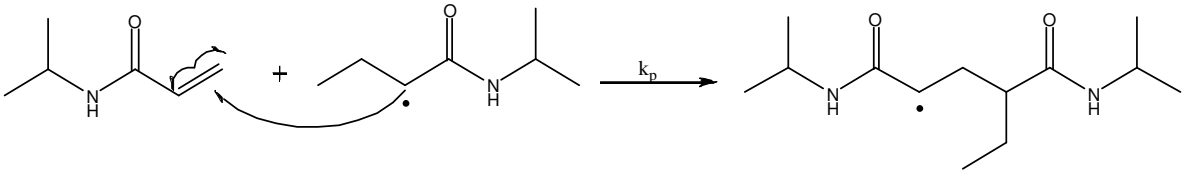

Figure 5.3. Propagation reaction of PNIPAM.

5.3.1. Conformational Study

5.3.1.1. Conformational Analysis of the Reactants. Conformational analysis showed that the cis conformer of the monomer, M1 (Figure 5.4a), was found to be more stable than the trans conformer M2 (Figure 5.4b) by 1.69 kcal/mol. The syn conformer of NIPAM radical, R1 (Figure 5.4c) was preferred over the anti conformer R2 (Figure 5.4d) by 1.53 kcal/mol. Also, the dipole moment of M1 was calculated as 3.60 D, whereas that of M2 was 3.92 D, indicating that the polarity of M1 is less than M2, so M1 is more stable based on dipole moments. Similarly, R1 has a dipole moment of 3.56 D and R2 has a dipole of 4.27 D. So, R1 was preferred over R2. In all conformations the hydrogen atom of the isopropyl group has an interaction with the carbonyl oxygen of the monomer and the radical. Because of

this weak interaction and the steric effects, the carbonyl group interacts with the hydrogen of the isopropyl group.

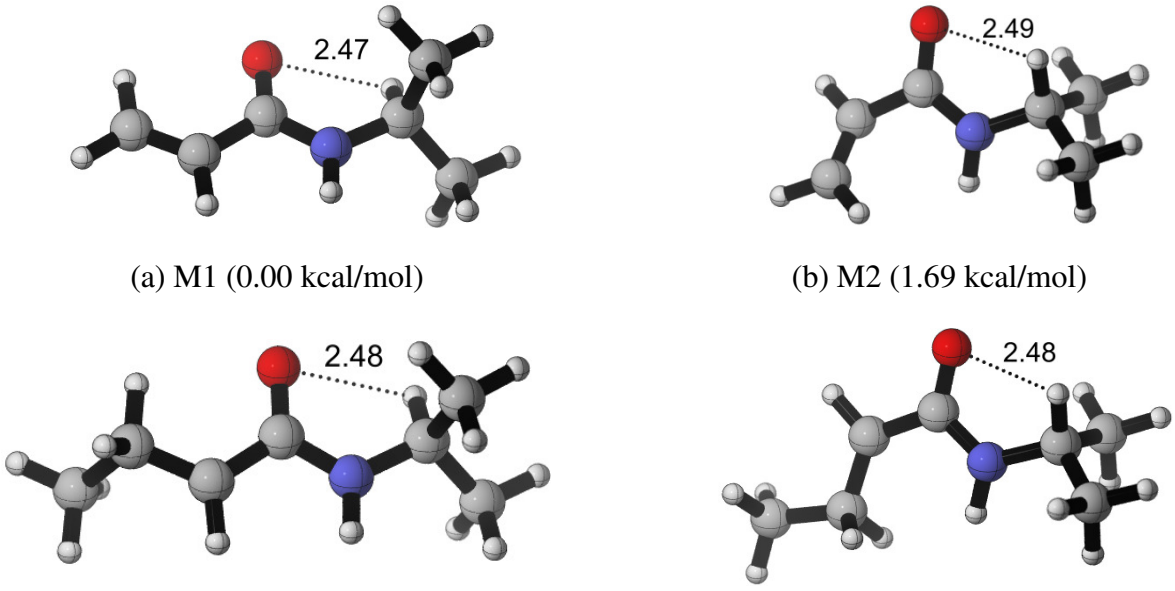

(a) M1 (0.00 kcal/mol) (b) M2 (1.69 kcal/mol)

(c) R1 (0.00 kcal/mol) (d) R2 (1.53 kcal/mol)

Figure 5.4. Conformational analysis of monomers and radicals.

5.3.1.2. Conformational Analysis of the Transition States. In Figure 5.5 and 5.6 the transition state geometries of the propagation reaction and the relaxed potential energy scan results for the isotactic and the syndiotactic transition states are depicted. Since the most stable geometry of the monomer was found as the cis conformer and that of NIPAM radical as the syn conformer, the transition states were modeled with these geometries. The potential energy scan was performed along the critical bond (C·---C(C=C)) for both transition states.

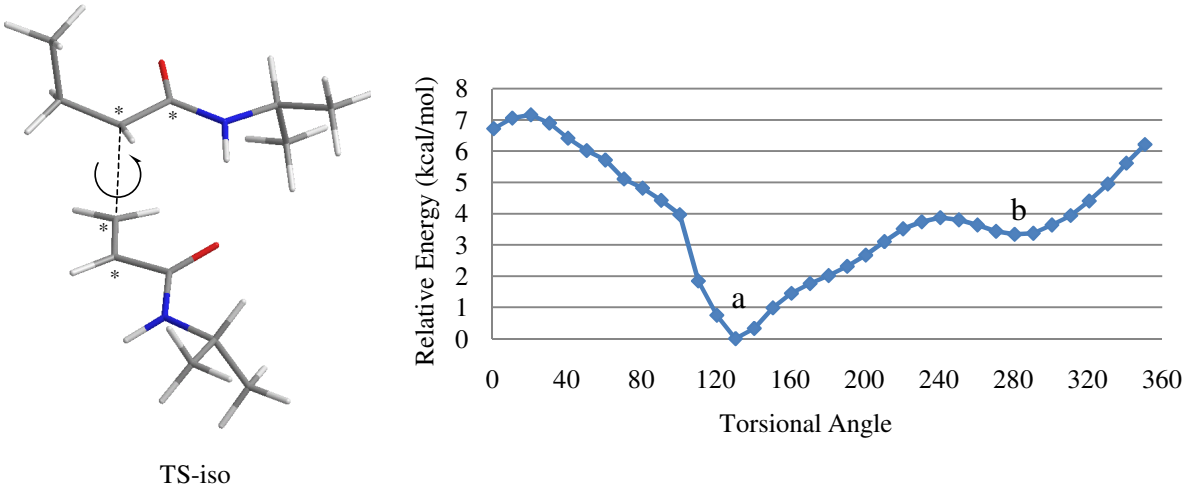

TS-iso

Figure 5.5. Potential energy scan for the isotactic transition state.

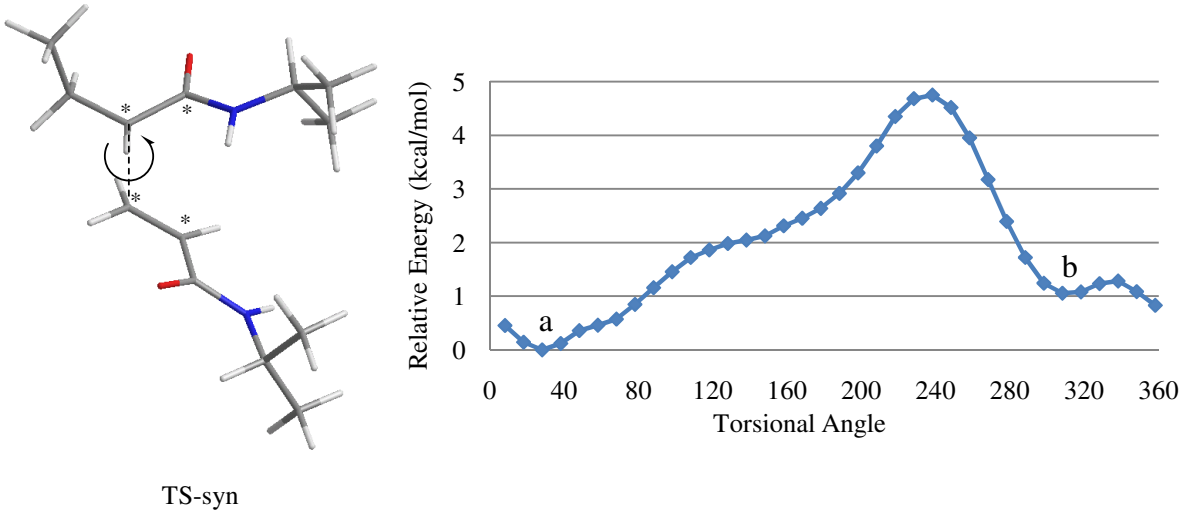

TS-syn

Figure 5.6. Potential energy scan for the syndiotactic transition state.

After the geometry optimization (B3LYP/6-31+G(d)) of the two minima (a and b) in the potential energy scan of the isotactic transition state (Figure 5.5), geometries in the Figure 5.7 were obtained. According to the relative energies, TS-iso-a having a hydrogen bonding interaction between the N-H proton of the radical and the carbonyl oxygen of the monomer was more stable than TS-iso-b by 2.74 kcal/mol. Also the dihedral angle C1-C2-C3-C4 in TS-iso-a has a value of 130.7^0, whereas that of TS-iso-b has 284.2^0.

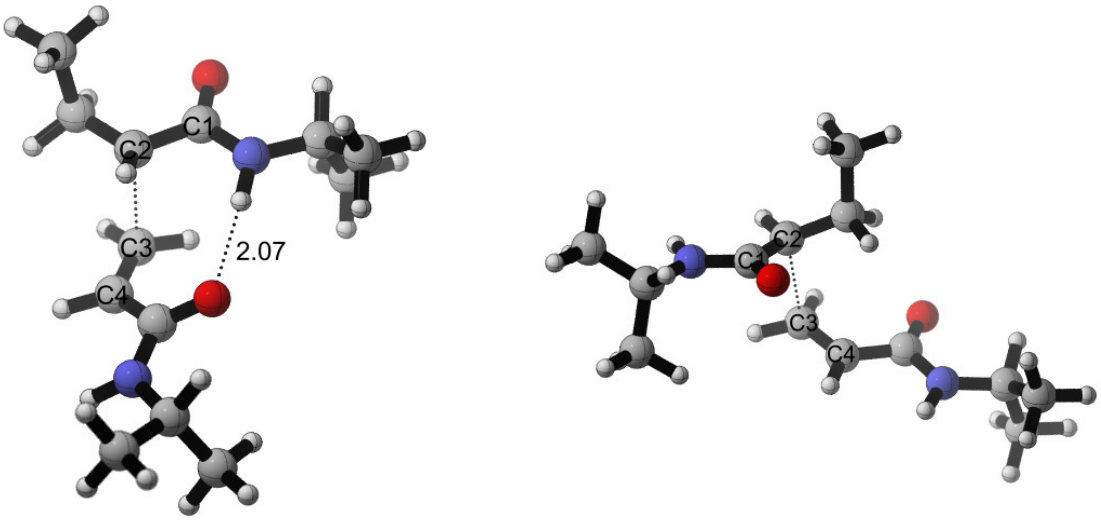

TS-iso-a (0.00 kcal/mol) TS-iso-b (2.74 kcal/mol)

Figure 5.7. Transition states obtained from the optimization (B3LYP/6-31+G(d)) of two minima in Figure 5.5.

Energies of the two minima (a and b) in the potential energy scan of TS-syn (Figure 5.6) were very close to each other. After the geometry optimization of these minima, TS-syn-b (Figure 5.8) having a hydrogen bonding interaction as in the TS-iso-a had a lower energy. Also the dihedral angle C1-C2-C3-C4 in TS-syn-a had a value of 48.1^0, whereas that of TS-syn-b had 29.2^0.

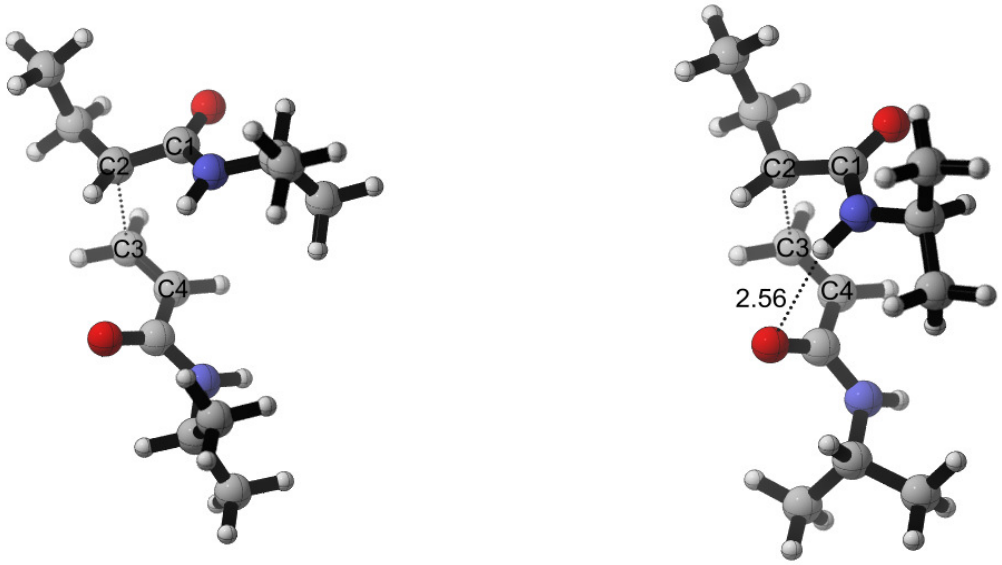

TS-syn-a (0.06 kcal/mol) TS-syn-b (0.00 kcal/mol)

Figure 5.8. Transition states obtained from the optimization (B3LYP/6-31+G(d)) of two minima in Figure 5.6.

5.3.2. Solvent Effect

5.3.2.1. Without Explicit Methanol Molecules. The free energy of activation ($\Delta G^{\#}$) and the propagation rate constant (k_p) for the propagation step of NIPAM polymerization were calculated at 300 K. Gas phase optimizations were done at B3LYP/6-31+G(d) level of theory and energies for transition states were also found at B3LYP/6-311+G(d,p) level with single point calculations. Solvent calculations were done with conductor-like polarizable continuum model (CPCM) by choosing methanol as solvent. All the results are tabulated in Table 5.1.

Table 5.1. Free energy barriers ($\Delta G^{\#}$) and the ratio of propagation rate constants for the transition states without explicit methanol molecules.

Methodology	TS-iso	TS-syn	$k_{p\ (syn)} / k_{p\ (iso)}$
	$\Delta G^{\#}$ (kcal/mol)	$\Delta G^{\#}$ (kcal/mol)	
B3LYP/6-31+G(d)	17.73	18.21	0.447
B3LYP/6-311+G(d,p)	18.30	18.88	0.377
B3LYP/6-311+G(d,p) (CPCM)	14.52	14.86	0.585

In Table 5.1, the ratio of the propagation rate constants of the syndiotactic and the isotactic transition states ($k_{p\ (syn)} / k_{p\ (iso)}$) gets larger when CPCM with methanol was used. According to an experimental study [77], addition of methanol molecules increases the syndiotacticity and accelerates the propagation reaction. Our CPCM results showed that choosing methanol as a medium lowers the free energy barriers, thereby the reaction rates, especially that of the syndiotactic transition state.

5.3.2.2. With Explicit Methanol Molecules. To see the effect of methanol addition on the tacticity and the rate of the propagation step in PNIPAM polymerization, one explicit methanol molecule was added first to the reactants. Possible conformations of the methanol molecules around monomer and the NIPAM radical are shown in Figure 5.9 and 5.10 respectively. Stabilization energies of the molecules with the methanol in terms of electronic energy were calculated as the difference of the electronic energies of the molecule-methanol complex and molecule and solvent separately. Conformers where O-H proton of the methanol has a hydrogen bonding interaction with the carbonyl oxygen of monomer and the radical were preferred.

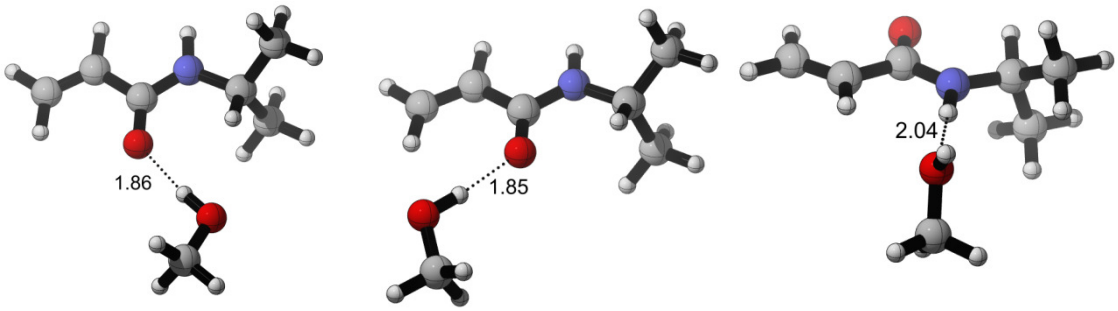

M1-MeOH (-6.16 kcal/mol) M2-MeOH (-6.14 kcal/mol) M3-MeOH (-4.18 kcal/mol)

Figure 5.9. Conformations of methanol around monomer and stabilization energies.

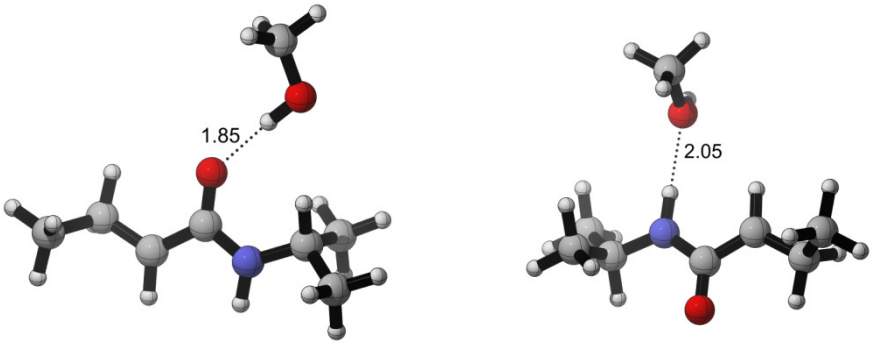

R1-MeOH (-6.37 kcal/mol) R2-MeOH (-3.89 kcal/mol)

Figure 5.10. Conformations of methanol around radical and stabilization energies.

Preference for the carbonyl oxygen for the methanol assistance can be explained by the hydrogen bond distances in Figures 5.9 and 5.10. In all the geometries where O-H hydrogen of the methanol coordinates to the carbonyl oxygen (M1-MeOH, M2-MeOH, R1-MeOH) hydrogen bond distances are smaller than those of M3-MeOH and R2-MeOH. Stronger hydrogen bonding interactions in these geometries render them more stable.

The same conformational analysis was done for the transition state structures. One explicit methanol molecule was added to the several positions in the isotactic and the

syndiotactic transition states (Figure 5.11). Bridging interaction of the methanol molecule was preferred and the kinetic results for these transition states are tabulated in Table 5.2.

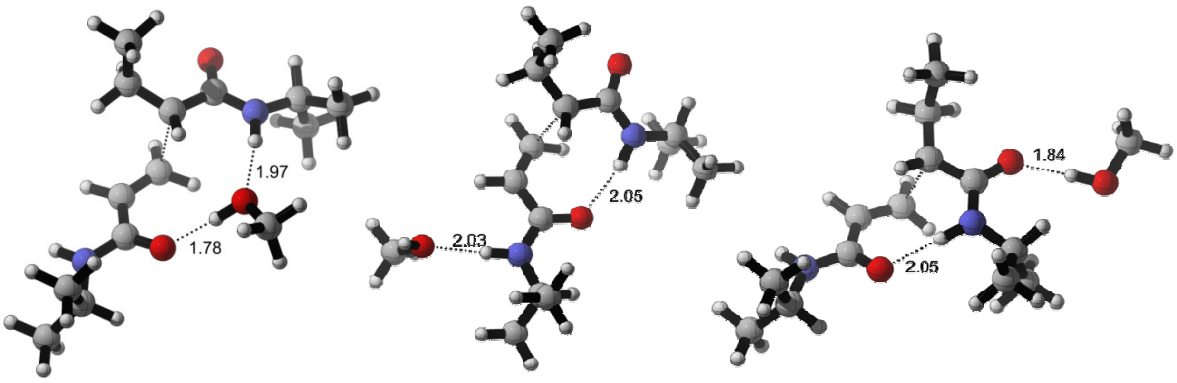

TS1-iso-MeOH (-10.01 kcal/mol) | TS2-iso-MeOH (-4.56 kcal/mol) | TS3-iso-MeOH (-6.89 kcal/mol)

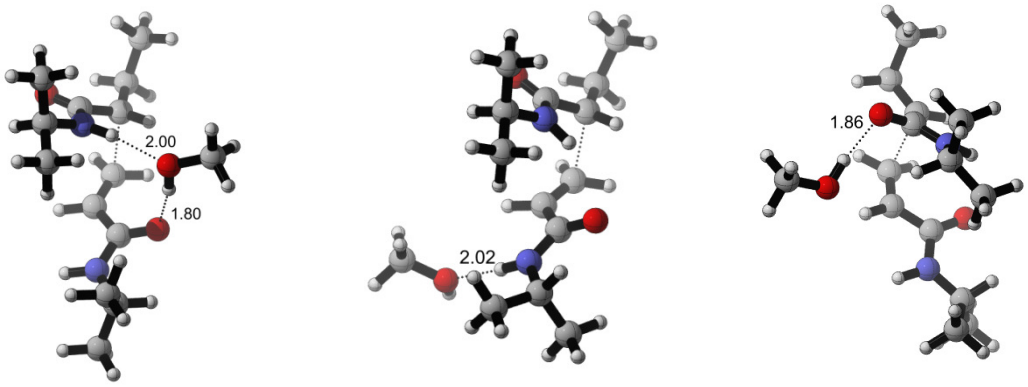

TS1-syn-MeOH (-10.14 kcal/mol) | TS2-syn-MeOH (-4.45 kcal/mol) | TS3-syn-MeOH (-7.56 kcal/mol)

Figure 5.11. Conformational analysis for the transition state structures with one explicit methanol.

As shown in Figure 5.11, for both the isotactic and the syndiotactic transition states, the ones having a bridging interaction with the methanol molecule are favored. Hydrogen bond distances for TS1-iso-MeOH and TS1-syn-MeOH are shorter than the ones in the others. Also, bridging interactions loosens the intermolecular hydrogen bonding

interactions in the transition states, thereby rendering them more stable. The preference for the bridging interactions can be explained by the charges on the carbonyl oxygens and the N-H protons in the transition states (Figure 5.12).

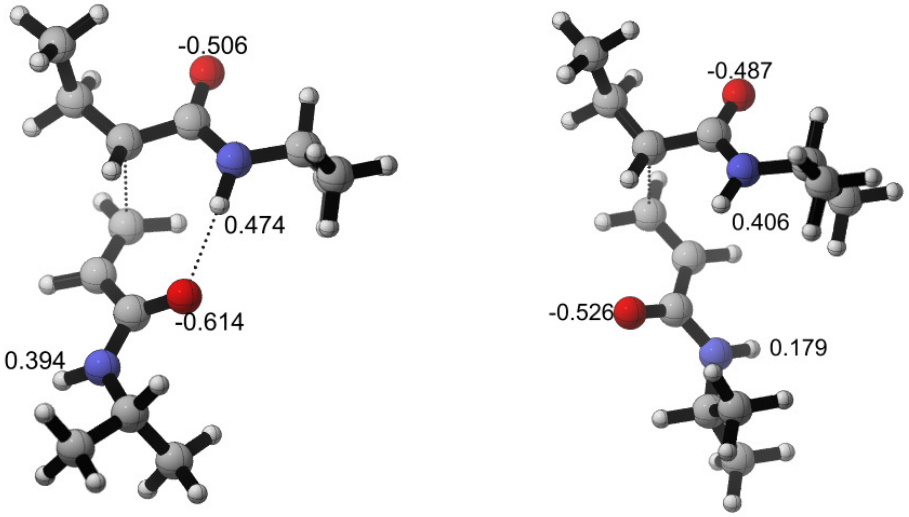

TS-iso-a TS-syn-b

Figure 5.12. Charges on the oxygen and the N-H hydrogens of the transition states.

Carbonyl oxygen which is hydrogen-bonded to the N-H hydrogen in TS-iso-b (Figure 5.12) is more negatively charged than the other oxygen. So, the carbonyl oxygen in the bridging position is more susceptible to interaction with methanol molecule. Similarly, the same position in TS-syn-b is more favorable for solvent coordination because of the more positive and the more negative charges on the N-H proton of the radical and the oxygen on the monomer, respectively.

Table 5.2. Free energy barriers ($\Delta G^{\#}$) and the ratio of propagation rate constants for the transition states with one explicit methanol molecule.

Methodology	TS-iso	TS-syn	$k_{p\ (syn)} / k_{p\ (iso)}$
	$\Delta G^{\#}$ (kcal/mol)	$\Delta G^{\#}$ (kcal/mol)	
B3LYP/6-31+G(d)	14.74	17.56	0.009
B3LYP/6-311+G(d,p)	15.38	18.37	0.006
B3LYP/6-311+G(d,p) (CPCM)	13.47	16.10	0.012

In the presence of one explicit methanol molecule and going from the gas phase calculation at B3LYP/6-311+G(d,p) level to mixed solvation with CPCM, $k_{p\ (syn)} / k_{p\ (iso)}$ ratio increases (Table 5.2) as in the previous case without any explicit solvent molecule (Table 5.1).

Transition state structures with two explicit methanol molecules are depicted in Figure 5.13 and the free energy of activation barriers ($\Delta G^{\#}$) for these geometries are given in Table 5.3.

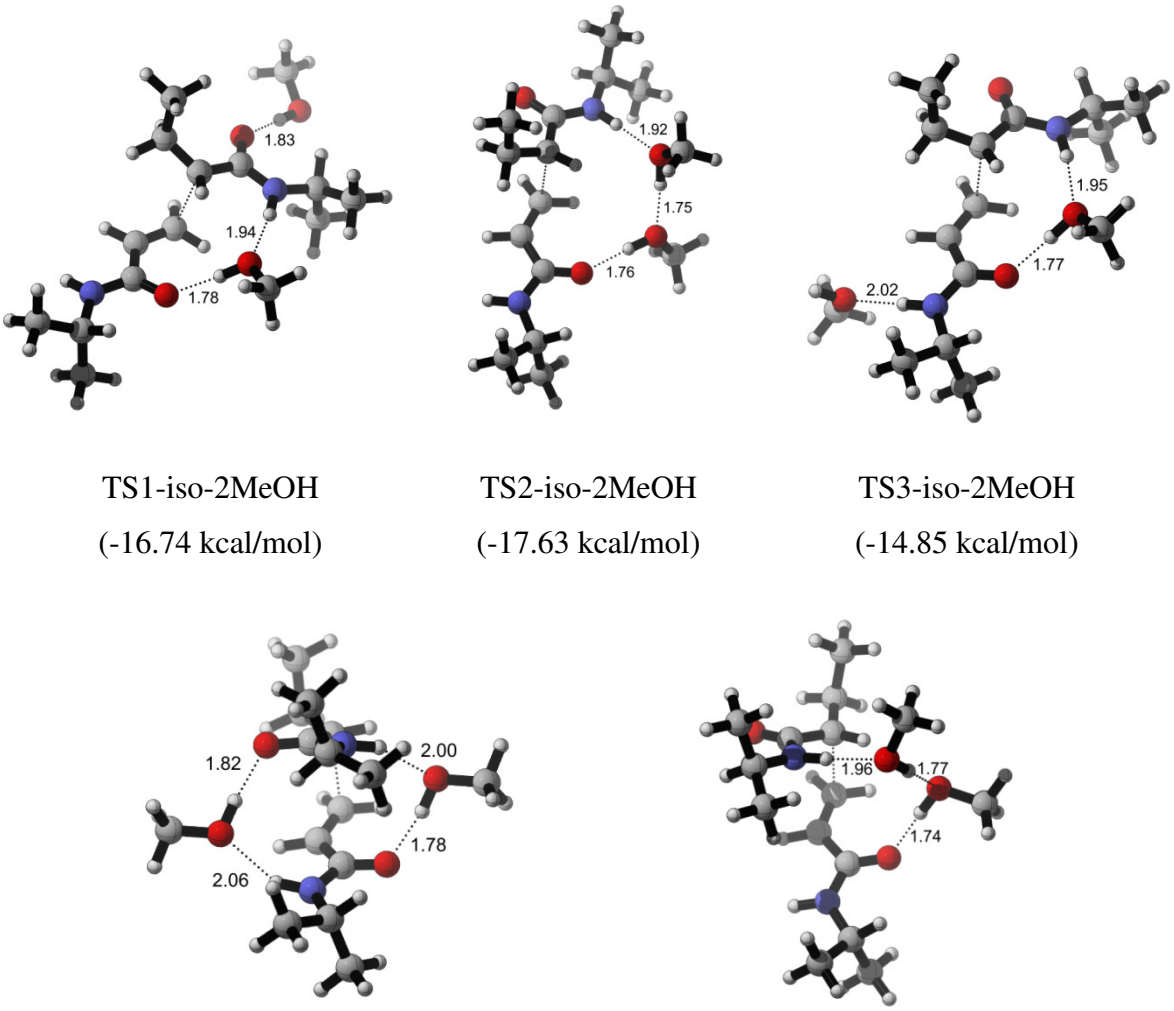

TS1-iso-2MeOH (-16.74 kcal/mol)

TS2-iso-2MeOH (-17.63 kcal/mol)

TS3-iso-2MeOH (-14.85 kcal/mol)

TS1-syn-2MeOH (-20.43 kcal/mol)

TS2-syn-2MeOH (-18.57 kcal/mol)

Figure 5.13. Conformational analysis for the transition state structures with two methanols.

Among the isotactic transition states with two solvent molecules, TS2-iso-2MeOH has the lowest stabilization energy, where both methanol molecules form a nice bridge on one side of the transition state. Whereas for the syndiotactic transition states, TS1-syn-2MeOH is more favorable where two solvent molecules separately form bridges on both sides (Figure 5.13).

Table 5.3. Free energy barriers ($\Delta G^{\#}$) and the ratio of propagation rate constants for the transition states with two explicit methanol molecules.

Methodology	TS-iso	TS-syn	$k_{p\ (syn)} / k_{p\ (iso)}$
	$\Delta G^{\#}$ (kcal/mol)	$\Delta G^{\#}$ (kcal/mol)	
B3LYP/6-31+G(d)	14.57	16.00	0.092
B3LYP/6-311+G(d,p)	13.56	16.99	0.003
B3LYP/6-311+G(d,p) (CPCM)	13.47	15.57	0.029

Increase in the number of explicit solvent molecules decreases the reaction barriers furthermore (Table 5.3). Also, when we compare the mixed solvation results with one and two explicit methanol molecules, the ratio of the propagation rate constants of the syndiotactic and the isotactic transition states gets larger. Also, the stabilization energies of the complexes become more and more negative as the number of explicit solvent molecules increases (Figures 11 and 13).

5.4. Conclusions and Future Work

The effect of methanol as a solvent in the propagation reaction of the poly(N-isopropylacrylamide (PNIPAM) was studied and discussed. For this purpose, implicit, explicit, and mixed solvation models were used. The conductor-like polarizable continuum model (CPCM) was chosen as the implicit solvation method. For the mixed solvent calculations, first the solute was solvated with one and two methanol molecules explicitly, then implicit calculations were done for these complexes by selecting the medium as methanol.

Our results showed that solvation with methanol decreases the reaction barriers, thereby increasing the reaction rates. Also, as the number of explicit solvent molecules increases, the propagation rate constant for the syndiotactic transition state increases more, so higher $k_{p\ (syn)} / k_{p\ (iso)}$ ratio was obtained. In the transition state geometries, the solvent molecules prefer to coordinate with the reactants at the bridging position. Because bridging interactions loosen the intermolecular hydrogen-bonds, transition state structures become more stable and favorable to form products.

For the further understanding of the solvent effect on the propagation and the tacticity of poly(N-isopropylacrylamide) (PNIPAM), the number of explicit methanol molecules will be increased and the number of solvent molecules that stabilizes the transition state structures will be investigated. The tacticity of the polymerization under these conditions will be tested. Experimentally, m and r dyad content in the presence of four-fold amount of methanol in radical polymerization of NIPAM at 0^0C was found as 40 and 60 %, respectively [77]. By changing the temperature and increasing the number of solvent molecules, the experimental findings will be rationalized.

REFERENCES

1. Matyjaszewski, K. and T. P. Davis, *Handbook of Radical Polymerization*, Wiley-Interscience Publication, New York, 2002.

2. Billmeyer F. W., *Textbook of Polymer Science*, Willey-Interscience Publication, Singapore, 1984.

3. Odian, G., *Principles of Polymerization*, Wiley-Interscience Publication, New York, 1991.

4. Robello, D. R., *Introduction to Polymer Chemistry*, http.//www.chem.rochester.edu /~chem421/frpolym.htm, 2002.

5. Beuermann, S. and M. Buback, “Rate Coefficients of Free Radical Polymerization Deduced from Pulsed Laser Experiments”, *Prog. Polym. Sci.*, Vol. 27, pp. 191-254, 2002.

6. Atkins P. and J. Paulo, *Physical Chemistry*, Oxford University Press, New York, 2002.

7. Heuts, J. P. A., T. P. Davis and G. T. Russell, "Comparison of the Mayo and Chain Length Distribution Procedures for the Measurement of Chain Transfer Constants", *Macromolecules*, Vol. 32, pp. 6019-6030, 1999.

8. Parr, R. G. and W. Yang, *Density Functional Theory of Atoms and Molecules*, Oxford University Press, New York, 1989.

9. Becke, A. D., “Density-Functional Exchange Energy Approximation with Correct Asymptotic Behavior”, *Phys. Rev. A.*, Vol. 38, pp. 3098-3103, 1988.

10. Becke A. D., “A New Mixing of Hartree-Fock and Local Density Functional Theories”, *J. Chem. Phys*., Vol. 38, 1372-1377, 1993.

11. Handy, N. C., “Density Functional Theory”, in: B. O. Roos (ed.), Lecture Notes in Quantum Chemistry, Vol. 2, pp. 91-123, Springer-Verlag, Berlin, 1994.

12. Leach, A. R., *Molecular Modelling Principles and Applications*, Prentice Hall, England, 2001.

13. Lee, C., W. Yang and R. G. Parr, “Development of Colle-Salvatti Correlation Energy Formula into a Functional of the Electron Density”, *Phys. Rev. B*, Vol. 37, pp. 785-789, 1988.

14. Becke, A. D., “Density Functional Thermochemistry. III. The Role of Exact Exchange”, *J. Chem. Phys*., Vol. 98, pp. 5648-5652, 1993.

15. Pauling, L. J., “The Nature of the Chemical Bond. IV. The Energy of Single Bonds and the Relative Electronegativity of Atoms”, *J. Am. Chem. Soc*., Vol. 54, pp. 3570-3582, 1932.

16. Tapia, O. and J. Bertrán, *Solvent Effects and Chemical Reactivity*, Kluwer Academic Publishers, The Netherlands, 1996.

17. Cramer, C. J. and D. G. Truhlar, "Implicit Solvation Models: Equilibria, Structure, Spectra, and Dynamics", *Chem. Rev.*, Vol. 99, pp. 2162-220, 1999.

18. Tomasi, J., B. Mennucci and R. Cammi, "Quantum Mechanical Continuum Solvation Models", *Chem. Rev.*, Vol. 105, pp. 2999-3093, 2005.

19. Barone, V., M. Cossi and J. Tomasi, "Geometry Optimization of Molecular Structures in Solution by the Polarizable Continuum Model", *J. Comp. Chem.*, Vol.19, pp. 404-417, 1998.

20. Barone, V. and M. Cossi, "Quantum Calculation of Molecular Energies and Energy Gradients in Solution by a Conductor Solvent Model", *J. Phys. Chem. A*, Vol. 102, pp. 1995-2001, 1998.

21. Matyjaszewski, K., *Advances in Controlled/Living Radical Polymerization*, Oxford University Press, Washington, 2003.

22. Satoh, K. and M. Kamigaito, "Stereospecific Living Radical Polymerization: Dual Control of Chain Length and Tacticity for Precision Polymer Synthesis", *Chem. Rev.*, Vol. 109, pp. 5120-5156, 2009.

23. Ansong, O., S. Jansen, Y. Wei, G. Pomrink, H. Lui, A. Patel and S. Li, "Accelerated controlled radical polymerization of methacrylates", *Polym. Int.*, Vol. 58, pp. 54-65, 2009.

24. Kwak, Y., R. Nicolay and K. Matyjaszewski, "Concurrent ATRP/RAFT of Styrene and Methyl Methacrylate with Dithioesters Catalyzed by Copper (1) Complexes", *Macromolecules*, Vol. 41, pp. 6602-6604, 2008.

25. Zetterlund, P. B., Y. Kagawa and M. Okubo, "Controlled/Living Radical Polymerization in Dispersed Systems", *Chem. Rev.*, Vol. 108, pp. 3747-3794, 2008.

26. Ishızu, K., H. Katsuhara and K. Itoya, "Controlled Radical Polymerization of Methacrylic Acid Initiated by Diethyldithio-carbamate-Mediated Iniferter", *Journal of Polymer Science: Part A: Polymer Chemistry*, Vol. 43, pp. 230-233, 2005.

27. Gridnev, A. A. and S. D. Ittel, "Catalytic Chain Transfer in Free-radical Polymerizations", *Chem. Rev.*, Vol. 101, pp. 3611-3659, 2001.

28. Valdebenito, A. and M. V. Encinas, "Chain Transfer Agents in Vinyl Polymerizations Photo-induced by Bimolecular Photoinitiators", *Journal of Photochemistry and Photobiology A: Chemistry*, Vol. 194, pp. 206–211, 2008.

29. Mayo, F. R., "Chain Transfer in the Polymerization of Styrene: The Reaction of Solvents with Free Radicals", *J. Am. Chem. Soc.*, Vol. 65, pp. 2324–2329, 1943.

30. Brandrup, J., E. H. Immergut and E. A. Grulke, *Polymer Handbook*, Wiley-Interscience: Hoboken, NJ, 1999**.**

31. Pross, A. and S. Shaik, "A Qualitative Valence-Bond Approach to Organic-Reactivity", *Acc. Chem. Res*., Vol. 16, pp. 363–370, 1983.

32. Pross, A., H. Yamataka and S. J. Nagase, "Reactivity in Radical Abstraction Reactions-Application of the Curve Crossing Model", *Phys. Org. Chem.*, Vol. 4, pp. 135–140, 1991.

33. Beare, K. D. and M. L. Coote, "What Influences Barrier Heights in Hydrogen Abstraction from Thiols by Carbon-Centered Radicals? A Curve-Crossing Study", *J. Phys. Chem. A*., Vol. 108, pp. 7211–7221, 2004.

34. Rong, X. X., H. Pan and W. R. Jr. Dolbier, "Reactivity of Fluorinated Alkyl Radicals in Solution - Some Absolute Rates of Hydrogen-Atom Abstraction and Cyclization", *J. Am. Chem. Soc*., Vol. 116, pp. 4521–4522, 1994.

35. Vijayalakshmi, N., M. Reddy, S. V. Naidu, T. Ramanjappa and P. Appalanaidu, "Immiscibility of Silicone Rubber and Polymethylmethacrylate", *International Journal of Polymeric Materials*, Vol. 57, pp. 709-716, 2008.

36. John, K. S., *Introduction to Polymer Chemistry*, University of Iowa Press, Iowa, 1962.

37. Gaussian 03, Revision B.05, Frisch, M. J., Gaussian, Inc., Wallingford CT, 2004.

38. Degirmenci, I., D. Avcı, V. Aviyente, K. Van Cauter, V. Van Speybroeck and M. Waroquier, "Density Functional Theory Study of Free-Radical Polymerization of

Acrylates and Methacrylates: Structure-Reactivity Relationship", *Macromolecules*, Vol. 40, pp. 9590–9602, 2007.

39. Degirmenci, I., V. Aviyente, V. Van Speybroeck and M. Waroquier, "DFT Study on the Propagation Kinetics of Free-Radical Polymerization of alpha-Substituted Acrylates", *Macromolecules*, Vol. 42, pp. 3033–3041, 2009.

40. Van Cauter, K., V. Van Speybroeck, P. Vansteenkiste, M. F. Reyniers and M. Waroquier, "Ab Initio Study of Free Radical Polymerization: Polyethylene Propagation Kinetics", *ChemPhysChem*, Vol. 7, pp. 131–140, 2006.

41. Speybroeck, V., K. Van Cauter, B. Coussens and M. Waroquier, "Ab Initio Study of Fre-Radical Polymerizations: Cost-Effective Methods to Determine the Reaction Rates", *ChemPhysChem*, Vol. 6, pp. 180–189, 2005.

42. Gomez-Balderas, R., M. L. Coote, D. J. Henry and L. J. Radom, "Reliable Theoretical Procedures for Calculating the Rate of Methyl Radical Addition to Carbon-Carbon Double and Trile Bonds", *Phys. Chem. A*, Vol. 108, pp. 2874–2883, 2004.

43. Coote, M. L., "Reliable Theoretical Procedures for the Calculation of Electronic-Structure Information in Hydrogen Abstraction Reactions", *J. Phys. Chem. A*, Vol. 108, pp. 3865–3872, 2004.

44. Smith, D. M., A. Nicolaides, B. T. Golding and L. Radom, "Ring Opening of the Cyclopropylcarbinyl Radical and Its N- and O-Substituted Analogues. A Theoretical Examination of Very Fast Unimolecular Reactions", *J. Am. Chem. Soc.*, Vol. 120, pp. 10223–10233, 1998.

45. Zhao, Y. and D. G. Truhlar, "Hybrid Meta Density Functional Theory Methods for Thermochemistry, Thermochemical Kinetics, and Noncovalent Interactions: The MPW1B95 and MPWB1K Models and Comparative Assessments for Hydrogen Bonding and Van Der Waals Interactions", *J. Phys. Chem. A*, Vol. 108, pp. 6908–6918, 2004.

46. Zhao, Y., N. E. Schultz and D. G. Truhlar, "Design of Density Functionals by Combining the Method of Constraint Satisfaction with Parametrization for Thermochemistry, Thermochemical Kinetics, and Noncovalent Interactions", *J. Chem. Theory Comput.,* Vol. 2*,* pp. 364-382, 2006.
47. Van Speybroeck, V., D. Van Neck, M. Waroquier, S. Wauters, M. Saeys and G. B. Marin, "Ab Initio Study of Radical Addition Reactions: Addition of a Primary Ethylbenzene Radical to Ethene (I)", *J. Phys. Chem. A*, Vol. 104, pp. 10939-10950, 2000.
48. Sabbe, M. K., A. G. Vandeputte, M. F. Reyniers, V. Van Speybroeck, M. Waroquier and G. B. Marin, "Ab Initio Thermochemistry and Kinetics for Carbon-Centered Radical Addition and beta-Scission Reactions", *J. Phys. Chem. A*, Vol. 111, pp. 8416-8428, 2007.
49. Van Cauter, K., K. Hemelsoet, V. Van Speybroeck, M. F. Reyniers and M. Waroquier, "Comparative Study of Kinetics and Reactivity Indices of Free Radical Polymerization Reactions", *International Journal of Quantum Chemistry*, Vol. 102, pp. 454–460, 2005.
50. Hemelsoet, K., V. Van Speybroeck, D. Moran, G. B. Marin, L. Radom and M. Waroquier, "Thermochemistry and Kinetics of Hydrogen Abstraction by Methyl Radical From Polycyclic Aromatic Hydrocarbons", *J. Phys. Chem.* A, Vol. 110, pp. 13624-13631, 2006.
51. Van Speybroeck, V., K. Hemelsoet, B. Minner, G. Marin and M. Waroquier, "Modeling Elementary Reactions in Coke Formation From First Principles", *Molecular Simulation*, Vol. 33, pp. 879–887, 2007.
52. Vandeputte, A. G., M. K. Sabbe, M. F. Reyniers, V. Van Speybroeck, M. Waroquier and G. B. Marin, "Theoretical Study of the Thermodynamics and Kinetics of Hydrogen Abstractions from Hydrocarbons", *J. Phys. Chem. A*, Vol. 111, pp. 11771-11786, 2007.

53. Coote, M. L., M. A. Collins and L. Radom, "Calculation of Accurate Imaginary Frequencies and Tunneling Coefficients for Hydrogen Abstraction Reactions Using IRCmax", *Mol. Phys*., Vol. 101, pp. 1329-1338, 2003.

54. Wigner, E. P., *Z. J. Phys. Chem. B*, Vol. 19, p. 203, 1932.

55. Eckart, C., "The Penetration of a Potential Barrier by Electrons", *Phys. Rev.,* Vol. 35, pp. 1303-1309, 1930.

56. Hemelsoet, K., V. Van Speybroeck and M. Waroquier, "A DFT-Based Investigation of Hydrogen Abstraction Reactions from Methylated Polycyclic Aromatic Hydrocarbons", *ChemPhysChem*., Vol. 9, pp. 2349–2358, 2008.

57. Da Silva, G., C. Chen and J. W. Bozzelli, "Bond Dissociation Energy of the Phenol O-H Bond from Ab Initio Calculations", *Chem. Phys. Lett.*, Vol. 424, pp. 42–45, 2006.

58. Blanksby, S. J. and G. B. Ellison, "Bond Dissociation Energies of Organic Molecules", *Acc. Chem. Res.,* Vol. 36, pp. 255-263, 2003.

59. Tomasi, J., B. Mennucci and E. Cance`s, "The IEF Version of the PCM Solvation Method: An Overview of a New Method Addressed to Study Molecular Solutes at the QM Ab Initio Level", *Journal of Molecular Structure-THEOCHEM,* Vol. 464, pp. 211-226, 1999.

60. Cance`s, M. T., B. Mennucci and J. Tomasi, "A New Integral Equation Formalism for the Polarizable Continuum Model: Theoretical Background and Applications to Isotropic and Anisotropic Dielectrics", *J. Chem. Phys*., Vol. 107, pp. 3032-3041, 1997.

61. Mennucci, B. and J. Tomasi, "Continuum Solvation Models: A New Approach to the Problem of Solute's Charge Distribution and Cavity Boundaries", *J. Chem. Phys.,* Vol. 106, pp. 5151-5158, 1997.

62. Mennucci, B., E. Cance`s and J. Tomasi, "Evaluation of Solvent Effects in Isotropic and Anisotropic Dielectrics and in Ionic Solutions with a Unified Integral Equation Method: Theoretical Bases, Computational Implementation, and Numerical Applications", *J. Phys.Chem. B*, Vol. 101, pp. 10506-10517, 1997.

63. Valdebenito, A. and M. V. Encinas, "Thiophenols as Chain Transfer Agents in the Polymerization of Vinyl Monomers", *Polymer*, Vol. 46, pp. 10658–10662, 2005.

64. Liptak, M.D., K. G. Gross, P. G. Seybold, S. Feldgus and G. C. Shields, "Absolute pK(a) Determinations for Substituted Phenols", *J. Amer. Chem. Soc.*, Vol. 124, pp. 6421-6427, 2002.

65. Evans, M. A. M. and Polanyi, "Inertia and Driving Force of Chemical Reactions", *Trans. Faraday Soc*., Vol. 34*,* pp. 11-29, 1938.

66. Izgorodina, E. I., D. R. B. Brittain, J. L. Hodgson, E. H. Krenske, C. Y. Lin, M. Namazian and M. L. Coote, "Should Contemporary Density Functional Theory Methods be Used to Study the Thermodynamics of Radical Reactions?", *J. Phys. Chem. A*, Vol. 111, pp. 10754-10768, 2007.

67. Zhao, Y. and D. G. Truhlar, "How Well can New-Generation Density Functionals Describe the Energetics of Bond-Dissociation Reactions Producing Radicals?", *J. Phys. Chem. A,* Vol. 112, pp. 1095-1099, 2008.

68. Brittain, D. R. B., C. Y. Lin, A. T. B. Gilbert, E. I. Izgorodina, P. M. W. Gill and M. L. Coote, "The Role of Exchange in Systematic DFT Errors for Some Organic Reactions", *Phys. Chem. Chem. Phys.*, Vol. 11, pp. 1138–1142, 2009.

69. Pross, A., *Theoretical and Physical Principles of Organic Reactivity,* Wiley-Interscience, New York, 1995.

70. Hansch, C., A. Leo and R. W. Taft, "A Survey of Hammett Substituent Constants and Resonance and Field Parameters", *Chem. Rev*., Vol. 91, pp. 165-195, 1991.

71. Porter, N. A., T. R. Allen and R. A. Breyer, "Chiral Auxiliary Control of Tacticity in Free-Radical Polymerization", *J. Am. Chem, Soc*., Vol. 114, pp. 7676-7683, 1992.

72. Rimmer, S., I. Soutar and L. Swanson, "Switching the Conformational Behaviour of Poly(N-Isopropyl Acrylamide)", *Polym. Int*., Vol. 58, pp. 273-278, 2009.

73. Yin, Z., J. Zhang, L. Jiang and J. Zhu, "Thermosensitive Behavior of Poly(N-Isopropylacrylamide) and Release of Incorporated Hemoglobin", *J. Phys. Chem. C*, Vol. 113, pp. 16104-16109, 2009.

74. Safrany, A. and L. Wojnarovits, "First steps in radiation-induced hydrogel synthesis: radical formation and oligomerization in dilute aqueous N-isopropylacrylamide solutions", *Radiation Physics and Chemistry*, Vol. 67, pp. 707-715, 2003.

75. You, Y. Z. and D. Oupicky, “Synthesis of Temperature-Responsive Heterobifunctional Block Copolymers of Poly(ethylene glycol) and Poly(N-isopropylacrylamide)”, *Biomacromolecules*, Vol. 8, No. 1, pp. 98-105, 2007.

76. Ge, Z., D. Xie, D. Chen, X. Jiang, Y. Zhang, H. Liu and S. Liu, “Stimuli-Responsive Double Hydrophilic Block Copolymer Micelles with Switchable Catalytic Activity”, *Macromolecules*, Vol. 40, No. 10, pp. 3538-3546, 2007.

77. Hirano, T., Y. Okumura, H. Kitajima, M. Seno and T. Sato, "Dual roles of Alkyl Alcohols as Syndiotactic-Specificty Inducers and Accelerators in the Radical Polymerization of N-Isopropylacrylamide and Some Properties of Syndiotactic Poly(N-Isopropylacrylamide)", *Journal of Polymer Science: Part A: Polymer Chemistry*, Vol. 44, pp. 4450-4460, 2006.

78. Hirano, T., H. Ishizu, M. Seno and T. Sato, "Hydrogen-Bond-Assisted Isotactic-Specific Radical Polymerization of N-Isopropylacrylamide with Pyridine N-Oxide", *Polymer*, Vol. 46, pp. 10607-10610, 2005.

79. Hirano, T., H. Ishizu and T. Sato, "Metal-Free Isotactic-Specific Radical Polymerization of N-Isopropylacrylamide with Pyridine N-Oxide Derivatives: The Effect of Methyl Substituents of Pyridine N-Oxide on the Isotactic Specificity and the Proposed Mechanism for the Isotactic-Specific Radical Polymerization", *Polymer*, Vol. 49, pp. 438-445, 2008.

80. Hirano, T., H. Miki, M. Seno and T. Sato, "Effect of Polymerization Conditions on the Syndiotactic-Specificity in Radical Polymerization of N-Isopropylacrylamide and Fractionation of the Obtained Polymer According to the Stereoregularity", *Polymer*, Vol. 46, pp. 5501-5505, 2005.

81. Hirano, T., S. Ishii, H. Kitajima, M. Seno and T. Sato, "Hydrogen-Bond-Assisted Stereocontrol in the Radical Polymerization of N-Isipropylacrylamide with Primary Alkyl Phosphate: The Effect of the Chain Length of the Straight Ester Group", *Journal of Polymer Science: Part A: Polymer Chemistry*, Vol. 43, pp. 50-62, 2005.

82. Barone, V. and M. Cossi, "Quantum Calculation of Molecular Energies and Energy Gradients in Solution by a Conductor Solvent Model", *J. Phys. Chem. A*, Vol. 102, pp. 1995-2001, 1998.

83. Weast, R. C., *Handbook of Chemistry and Physics*, Ed.; Chemical Rubber: Cleveland,OH, 1981.